



# Kent Academic Repository

Ahmad, Bilal, Friar, Emily P., Vohra, Muhammad Sufyan, Khan, Nasar, Serpell, Christopher J., Garrett, Michelle D., Loo, Jason Siau Ee, Fong, Isabel Lim and Wong, Eng Hwa (2023) *Hydroxylated polymethoxyflavones reduce the activity of pancreatic lipase, inhibit adipogenesis and enhance lipolysis in 3T3-L1 mouse embryonic fibroblast cells*. *Chemico-Biological Interactions*, 379 . ISSN 0009-2797.

## Downloaded from

<https://kar.kent.ac.uk/101195/> The University of Kent's Academic Repository KAR

## The version of record is available from

<https://doi.org/10.1016/j.cbi.2023.110503>

## This document version

Publisher pdf

## DOI for this version

## Licence for this version

CC BY (Attribution)

## Additional information

For the purpose of open access, the author has applied a CC BY public copyright licence to any Author Accepted Manuscript version arising from this submission.

## Versions of research works

### Versions of Record

If this version is the version of record, it is the same as the published version available on the publisher's web site. Cite as the published version.

### Author Accepted Manuscripts

If this document is identified as the Author Accepted Manuscript it is the version after peer review but before type setting, copy editing or publisher branding. Cite as Surname, Initial. (Year) 'Title of article'. To be published in **Title of Journal**, Volume and issue numbers [peer-reviewed accepted version]. Available at: DOI or URL (Accessed: date).

## Enquiries

If you have questions about this document contact [ResearchSupport@kent.ac.uk](mailto:ResearchSupport@kent.ac.uk). Please include the URL of the record in KAR. If you believe that your, or a third party's rights have been compromised through this document please see our [Take Down policy](https://www.kent.ac.uk/guides/kar-the-kent-academic-repository#policies) (available from <https://www.kent.ac.uk/guides/kar-the-kent-academic-repository#policies>).



## Research paper

# Hydroxylated polymethoxyflavones reduce the activity of pancreatic lipase, inhibit adipogenesis and enhance lipolysis in 3T3-L1 mouse embryonic fibroblast cells

Bilal Ahmad<sup>a</sup>, Emily P. Friar<sup>b</sup>, Muhammad Sufyan Vohra<sup>c</sup>, Nasar Khan<sup>d</sup>, Christopher J. Serpell<sup>b,\*\*</sup>, Michelle D. Garrett<sup>e</sup>, Jason Siau Ee Loo<sup>f</sup>, Isabel Lim Fong<sup>g</sup>, Eng Hwa Wong<sup>c,\*</sup>

<sup>a</sup> School of Biosciences, Faculty of Health and Medical Sciences Taylor's University Lakeside Campus, No1 Jalan Taylor's, 47500, Subang Jaya, Malaysia

<sup>b</sup> School of Chemistry and Forensic Science, Ingram Building, University of Kent, Canterbury, Kent, CT2 7NH, United Kingdom

<sup>c</sup> School of Medicine, Faculty of Health and Medical Sciences Taylor's University Lakeside Campus, No1 Jalan Taylor's, 47500, Subang Jaya, Malaysia

<sup>d</sup> R3 Medical Research, 10045 East Dynamite Boulevard Suite 260, Scottsdale, AZ, 85262, United States

<sup>e</sup> School of Biosciences, Stacey Building, University of Kent, Canterbury, Kent, CT2 7NJ, United Kingdom

<sup>f</sup> School of Pharmacy, Faculty of Health and Medical Sciences Taylor's University Lakeside Campus, No1 Jalan Taylor's, 47500, Subang Jaya, Malaysia

<sup>g</sup> Department of Paraclinical Sciences, Faculty of Medicine and Health Sciences, Universiti Malaysia Sarawak (UNIMAS), 94300, Kota Samarahan, Sarawak, Malaysia



## ARTICLE INFO

## Keywords:

HPMFs  
OBPMFs  
3T3-L1 adipocytes  
Pancreatic lipase  
Lipolysis

## ABSTRACT

Hydroxylated polymethoxyflavones (HPMFs) have been shown to possess various anti-disease effects, including against obesity. This study investigates the anti-obesity effects of HPMFs in further detail, aiming to gain understanding of their mechanism of action in this context. The current study demonstrates that two HPMFs; 3'-hydroxy-5,7,4',5'-tetramethoxyflavone (3'-OH-TetMF) and 4'-hydroxy-5,7,3',5'-tetramethoxyflavone (4'-OH-TetMF) possess anti-obesity effects. They both significantly reduced pancreatic lipase activity in a competitive manner as demonstrated by molecular docking and kinetic studies. In cell studies, it was revealed that both of the HPMFs suppress differentiation of 3T3-L1 mouse embryonic fibroblast cells during the early stages of adipogenesis. They also reduced expression of key adipogenic and lipogenic marker genes, namely peroxisome proliferator-activated receptor-gamma (PPAR $\gamma$ ), CCAAT/enhancer-binding protein  $\alpha$  and  $\beta$  (C/EBP  $\alpha$  and  $\beta$ ), adipocyte binding protein 2 (aP2), fatty acid synthase (FASN), and sterol regulatory element-binding protein 1 (SREBF 1). They also enhanced the expression of cell cycle genes, i.e., cyclin D1 (CCND1) and C-Myc, and reduced cyclin A2 expression. When further investigated, it was also observed that these HPMFs accelerate lipid breakdown (lipolysis) and enhance lipolytic genes expression. Moreover, they also reduced the secretion of proteins (adipokines), including pro-inflammatory cytokines, from mature adipocytes. Taken together, this study concludes that these HPMFs have anti-obesity effects, which are worthy of further investigation.

## 1. Introduction

Obesity is a worldwide health issue; it is now being recognized as a lifestyle disorder in the developing world, while its prevalence has already reached an alarming level in developed countries [1]. According to the 2017 Global Burden of Disease study, more than 4 million deaths were attributed to being overweight or obese that year. This trend of overweight and obesity was tracked from 1975 to 2016 and it was found to have increased more than 4-fold, from 4% to 18% globally [2,3].

Obesity contributes to metabolic syndrome, numerous cancers, cardiovascular disease, fatty liver, type II diabetes and insulin resistance [4,5]. It arises due to excess energy intake compared with energy expenditure, leading to excessive fat accumulation in adipose tissue [6]. Pancreatic lipase (PL) is crucial for the absorption and digestion of dietary fats [7, 8], and hydrolyzes 50–70% of the total dietary fats in the digestive system [9–11]. PL inhibition changes the absorption and digestion of ingested triglycerides and is therefore the most widely studied mechanism for screening anti-obesity agents [12,13]. In obesogenic

\* Corresponding author.

\*\* Corresponding author.

E-mail addresses: [C.J.Serpell@kent.ac.uk](mailto:C.J.Serpell@kent.ac.uk) (C.J. Serpell), [EngHwa.Wong@taylors.edu.my](mailto:EngHwa.Wong@taylors.edu.my) (E.H. Wong).

<https://doi.org/10.1016/j.cbi.2023.110503>

Received 8 December 2022; Received in revised form 13 April 2023; Accepted 18 April 2023

Available online 19 April 2023

0009-2797/© 2023 The Authors. Published by Elsevier B.V. This is an open access article under the CC BY license (<http://creativecommons.org/licenses/by/4.0/>).

conditions, excess fats are accumulated as triglycerides in the white adipocytes of white adipose tissue (WAT) [14]. Adipocytes are specialized cells within WAT which differentiate from mesenchymal stem cells through a well-orchestrated process known as adipogenesis [15], and have the ability to store excess energy (triglycerides) in lipid droplets. Various genes and transcriptional factors are involved in the differentiation of adipocytes and the accumulation of fats in mature adipocytes [16,17]. Therefore, inhibiting these genes and transcriptional factors and accelerating lipolysis is a crucial strategy in the fight against obesity and associated disorders.

Recently, we reported the anti-obesity effects of two similar fully methoxylated flavones [18] with no hydroxy groups. However, the bioactivities of flavones are dependent on the position and number of methoxy (-OCH<sub>3</sub>) and hydroxy (-OH) groups attached to the flavone skeleton [19]. Such differences in the distribution and number of chemical groups across the flavone skeleton play a crucial role in the wide range of pharmacological properties of flavones [20]. In addition, 3' and 4' positions on B ring of flavone skeleton are known to be the main sites of biotransformation [21]. So, in this study, two previously un-evaluated HPMFs (3'-OH-TetMF and 4'-OH-TetMF) having -OH groups on position 3' and 4' of B ring have been investigated for their anti-obesity effects. The results obtained in the present study showed that these two HPMFs significantly inhibit the activities of PL and inhibit adipogenesis during the early stages of 3T3-L1 differentiation. They significantly reduced adipogenic and lipogenic gene expression, i.e. PPAR $\gamma$ , C/EBP $\alpha$  and  $\beta$ , aP2, SREBF 1, and FASN. Furthermore, we observed that these HPMFs accelerate the release of glycerol from mature adipocytes (lipolysis) and enhance the expression of lipolytic genes such as adipose triglycerides lipase (ATGL), Hormone Sensitive Lipase (HSL) and monoglycerides lipase (MGL). In addition, these HPMFs also reduced the release of adipokines including pro-inflammatory cytokines from mature adipocytes.

## 2. Material and methods

### 2.1. Chemicals

Starting materials and reagents for chemical synthesis were purchased from Thermo Fisher Scientific. Dimethyl sulfoxide (DMSO), 3-(4,5-Dimethylthiazol-2-yl)-2,5-diphenyltetrazolium bromide (MTT), *p*-nitrophenyl butyrate (PNPB), Oil Red O powder, formalin, acetonitrile, isopropanol, phosphate buffer saline (PBS), and Tris-HCl were purchased from Sigma Aldrich, USA. Dulbecco's Modified Eagle Medium (DMEM), bovine calf serum (BCS), fetal bovine serum (FBS), trypsin, and Penicillin-Streptomycin Solution (Pen-Strep) were purchased from ATCC USA. Porcine PL (EC 3.1.1.3) was purchased from Sigma Aldrich USA. 3T3-L1 mouse fibroblast cells (Cat No. iCell-m066) were purchased from iCell Bioscience China.

### 2.2. Synthesis of HPMFs

#### 2.2.1. Synthesis of 3'-hydroxy-5,7,4',5'-tetramethoxyflavone (3'-OH-TetMF)

1-(2-Hydroxy-4,6-dimethoxyphenyl)ethanone (0.5 g, 2.55 mmol, 1 eq) was dissolved in methanol (15 mL) with 3,4-dimethoxy-5-hydroxybenzaldehyde (0.46 g, 2.55 mmol, 1 eq) and sodium hydroxide (0.16 g, 10.19 mmol, 4 eq). The solution was refluxed for 24 h at 80 °C. The solution was cooled to 5 °C and addition of a few drops of 6 M HCl caused a bright yellow precipitate to form. This was collected with filtration and washed with ice-cold methanol. Crude compound was purified using Biotage Isolera purification (eluent: Hexane:Ethyl Acetate over a gradient of 95:5 to 0:100; cartridge: Biotage SNAP KP-Sil 50g) to give a yellow product, chalcone 1. (0.44 g, 1.20 mmol, 47%) <sup>1</sup>H NMR (400 MHz, DMSO-*d*<sub>6</sub>)  $\delta$ <sub>H</sub> 13.43 (1H, s, OH - 2), 9.43 (1H, s, OH - 3'), 7.63–7.49 (2H, m, H - 3, H - 5), 6.84 (2H, dd, *J* = 8.8, 1.9, H - 2', H - 6'), 6.14 (2H, dd, *J* = 13.0, 2.3, H -  $\alpha$ , H -  $\beta$ ), 3.90 (3H, s, OCH<sub>3</sub> - 5) 3.82 (6H,

s, OCH<sub>3</sub> - 4, OCH<sub>3</sub> - 5') 3.71 (3H, s, OCH<sub>3</sub> - 4'). <sup>13</sup>C NMR (100 MHz, DMSO-*d*<sub>6</sub>)  $\delta$ <sub>C</sub> 191.8 (CO), 165.0 (COCH<sub>3</sub> - 4), 165.0 (COCH<sub>3</sub> - 6), 161.4 (COH - 2), 152.9 (COCH<sub>3</sub> - 5'), 150.4 (COH - 3'), 142.4 (C -  $\beta$ ), 138.2 (COCH<sub>3</sub> - 4'), 129.8 (C -  $\alpha$ ), 126.0 (C - 2'), 108.7 (C - 2'), 105.9 (COC), 104.0 (C - 6'), 93.5 (C - 3), 90.7 (C - 5), 59.6 (OCH<sub>3</sub> - 4'), 55.8 (OCH<sub>3</sub> - 4'), 55.4, 55.2 (OCH<sub>3</sub>). ESI-MS: *m/z* [M+H]<sup>+</sup> Calcd. 361.1, found 361.0, [M+Na]<sup>+</sup> Calcd. 383.1, found 383.0.

Iodine (70.40 mg, 0.28 mmols, 0.2 eq) was added to chalcone 1 (0.50 g, 1.39 mmols, 1 eq) in DMSO (10 mL). The solution was refluxed at 130 °C for 2 h, then cooled and poured into 10 [%w/w] sodium thiosulphate pentahydrate solution (50 mL) to give a cloudy orange solution with brown solid precipitate. This was filtered to collect precipitate. The aqueous solution extracted with ethyl acetate, and collected to give product as brown solid of 90% purity (0.37 g). The crude product was purified in batches using reverse phase Biotage Isolera purification (eluent: H<sub>2</sub>O + 0.1% formic acid: MeOH + 0.1% formic acid 5–100%, cartridge: Biotage SNAP Ultra C18 12g). This gave the desired flavone product 3'-OH-TetMF as an off-white powder. (0.18 g, 0.50 mmol, 48%). <sup>1</sup>H NMR (400 MHz, DMSO-*d*<sub>6</sub>)  $\delta$ <sub>H</sub> 9.54 (s, 1H, OH), 7.13 (dd, *J* = 11.6 Hz, 1.9 Hz, 2H, H-2',H-6'), 6.81 (d, *J* = 2.2 Hz, 1H, H-6), 6.69 (s, 1H, H- $\alpha$ ), 6.51 (d, *J* = 2.3 Hz, 1H, H-8) 3.90 (s, 3H, OCH<sub>3</sub>-5) 3.88 (s, 3H, OCH<sub>3</sub>-5') 3.83 (s, 3H, OCH<sub>3</sub>-7) 3.74 (s, 3H, OCH<sub>3</sub>-4'). <sup>13</sup>C NMR (100 MHz, DMSO-*d*<sub>6</sub>)  $\delta$ <sub>C</sub> 176.1 (CO), 164.1 (COCH<sub>3</sub> - 7), 160.7 (C - 2), 160.0 (COCH<sub>3</sub> - 5), 159.6 (C - 8a), 153.9 (COCH<sub>3</sub> - 5'), 151.3 (COH), 139.5 (COCH<sub>3</sub> - 4'), 126.5 (C - 1'), 108.7 (C - 4a), 108.2 (C - 2'), 107.7 (C -  $\alpha$ ), 102.0 (C - 6'), 96.7 (C - 6), 93.7 (C - 8), 60.5 (OCH<sub>3</sub> - 4'), 56.5 (OCH<sub>3</sub> - 5'), 56.5 (OCH<sub>3</sub> - 7), 56.4 (OCH<sub>3</sub> - 5). ESI-HRMS: *m/z* [M+H]<sup>+</sup> Calc'd. 359.1125, found 359.1167.

#### 2.2.2. Synthesis of 4'-hydroxy-5,7,3',5'-tetramethoxyflavone (4'-OH-TetMF)

Benzyl bromide (783  $\mu$ L, 6.59 mmol, 1.2 eq) was added to a solution of 4-hydroxy-3,5-dimethoxybenzaldehyde (1.00 g, 5.49 mmol, 1 eq) and potassium carbonate (1.52 g, 10.98 mmol, 2 eq) in DMF (10 mL). The mixture was stirred at rt for 24 h. The white emulsion formed was diluted with water (20 mL), causing product to precipitate. The remaining product was extracted using diethyl ether, and dried under reduced pressure to form an oil. The organic extracts were combined and dried to give the pure product, 4-(benzyloxy)-3,5-dimethoxybenzaldehyde 2, as a white solid (1.22 g, 4.48 mmol, 81%). <sup>1</sup>H NMR (400 MHz, DMSO-*d*<sub>6</sub>)  $\delta$ <sub>H</sub> 9.94 (1H, s, HCO), 7.51–7.34 (5H, m, ph-H), 7.31 (2H, s, H-2',H-6), 5.09 (2H, s, CH<sub>2</sub>), 3.91 (6H, s, OCH<sub>3</sub>). <sup>13</sup>C NMR (100 MHz, DMSO-*d*<sub>6</sub>)  $\delta$ <sub>C</sub> 192.3 (CHO), 154.0 (COCH<sub>3</sub>), 142.1 (COBn), 137.8 (CCH<sub>2</sub>), 132.3 (CCHO), 128.6, 128.5, 128.4 (C-Bn), 107.2 (CHCCHO), 74.5 (CH<sub>2</sub>), 56.6 (CH<sub>3</sub>). ESI-HRMS: *m/z* [M+Na]<sup>+</sup> Calc'd. 295.0946, found 295.0953.

1-(2-Hydroxy-4,6-dimethoxyphenyl)ethanone 2 (0.31 g, 1.59 mmol, 1 eq) was dissolved in methanol (20 mL) with 4-(benzyloxy)-3,5-dimethoxybenzaldehyde (0.43 g, 1.59 mmol, 1 eq) and sodium hydroxide (0.25 g, 6.34 mmol, 4 eq). The solution was refluxed for 24 h at 80 °C. Addition of a few drops of 6 M HCl caused a bright yellow precipitate to form. This was collected with filtration and washed with methanol to give product, chalcone 3, as a yellow solid (0.56 g, 1.24 mmol, 78%). <sup>1</sup>H NMR (400 MHz, DMSO-*d*<sub>6</sub>)  $\delta$ <sub>H</sub> 13.06 (1H, s, OH), 7.66–7.31 (7H, m, Bn-H, H-3, H-5), 7.05 (2H, s, H-2', H-4'), 6.15 (2H, dd, *J* = 9.8, 2, H- $\alpha$ , H- $\beta$ ), 4.95 (2H, CH<sub>2</sub>), 3.86 (3H, s, OCH<sub>3</sub>-4), 3.83 (6H, s, OCH<sub>3</sub>-3', OCH<sub>3</sub>-5'), 3.81 (3H, s, OCH<sub>3</sub>-6). <sup>13</sup>C NMR (100 MHz, DMSO-*d*<sub>6</sub>)  $\delta$ <sub>C</sub> 192.2 (CO), 165.0 (COCH<sub>3</sub> - 4), 164.5 (COCH<sub>3</sub> - 6), 161.4, (COH), 153.1 (COCH<sub>3</sub> - 3', COCH<sub>3</sub> - 5'), 142.5 (COCHCH), 138.2 (C-Bn), 137.4 (CCH<sub>2</sub>OBN), 130.3, 127.9, 127.8, 127.6 (Ph), 126.9 (C - 1'), 106.5 (C - 1), 105.7 (CH - 2', CH - 6'), 93.7 (CH - 3), 90.8 (CH - 5), 73.8 (CH<sub>2</sub>), 55.9, 55.9, 55.4 (OCH<sub>3</sub>). ESI-HRMS: *m/z* [M+H]<sup>+</sup> Calcd. 451.1751, found 451.1783.

Iodine (0.06 g, 0.25 mmols, 0.2 eq) was added to chalcone 3 (0.55 g, 1.23 mmols, 1 eq) in DMSO (10 mL). The solution was refluxed at 130 °C for 1 h, before being cooled and poured into 10% [%w/w] sodium thiosulphate pentahydrate solution (150 mL) to give a white precipitate.

This was collected by filtration and washed with water to give a white solid of 90% purity (0.56 g). The crude product was purified in batches using reverse phase Biotage Isolera purification (eluent: H<sub>2</sub>O + 0.1% formic acid: MeOH + 0.1% formic acid 5–100%, cartridge: Biotage SNAP Ultra C18 12g) to give the protected flavone **4**. This was used directly in the next step; purification of a small batch for analysis indicated a yield of 78%. <sup>1</sup>H NMR (400 MHz, DMSO-*d*<sub>6</sub>) δ<sub>H</sub> 7.47–7.33 (5H, m, Bn-H), 7.30 (2H, s, H-2', H-6'), 6.90 (1H, d, J = 2.3, H-8), 6.87 (1H, s, H-α), 6.50 (1H, d, J = 2.3, H-6), 5.00 (2H, s, CH<sub>2</sub>), 3.91 (3H, s, OCH<sub>3</sub>-5), 3.90 (6H, s, H-3', H-5'), 3.83 (3H, s, OCH<sub>3</sub>-7). <sup>13</sup>C NMR (100 MHz, DMSO-*d*<sub>6</sub>) δ<sub>C</sub> 175.8 (CO), 163.7 (COCH<sub>3</sub> - 7), 160.2 (C - β), 159.4 (COCH<sub>3</sub> - 5), 159.2 (C - 8a), 153.4 (COCH<sub>3</sub> - 3', COCH<sub>3</sub> - 5'), 138.9 (Bn - 1), 137.6 (COBn), 128.2 (Bn - 3, Bn - 5), 128.1 (Bn - 2, Bn - 6), 127.9 (Bn - 4), 126.3 (C - 1'), 108.3 (C - 4a), 108.2 (C - α), 103.5 (C - 2', C - 6'), 96.3 (C - 6), 93.5 (C - 8), 74.0 (CH<sub>2</sub>), 56.4 (OCH<sub>3</sub> - 3', OCH<sub>3</sub> - 5'), 56.1 (OCH<sub>3</sub> - 5, OCH<sub>3</sub> - 7). ESI-HRMS: *m/z* [M+H]<sup>+</sup> Calc'd. 449.1595, found 449.1662.

Boron trichloride (BCl<sub>3</sub>, 1560 μL, 1.0 M in CH<sub>2</sub>Cl<sub>2</sub>, 2 eq) was added to a stirred solution of **4** (0.35 g, 0.78 mmol, 1 eq) pentamethylbenzene (0.35 g, 2.34 mmol, 3 eq) in dry DCM (4 mL) via syringe at -84 °C dropwise over 10 min. After 15 min, due to complete consumption of starting material, the reaction was quenched with CHCl<sub>3</sub>:MeOH (10:1, 5 mL) and warmed to room temperature. A resulting orange solid was removed via filtration. The filtrate was concentrated under reduced pressure and purified using reverse phase Biotage Isolera purification (eluent: H<sub>2</sub>O + 0.1% formic acid: MeOH + 0.1% formic acid 5–100%, cartridge: Biotage SNAP Ultra C18 12g) to give the desired product, **4'** **OH-TetMF** as an off-white powder. (0.70 g, 0.20 mmol, 25%). <sup>1</sup>H NMR (400 MHz, DMSO-*d*<sub>6</sub>) δ<sub>H</sub> 9.11 (1H, s, OH), 7.29 (2H, s, H-2', H-6'), 6.90 (1H, d, J = 2.3, H-8), 6.78 (1H, s, H-α), 6.50 (1H, d, J = 2.3, H-6), 3.91 (3H, s, OCH<sub>3</sub>-5), 3.88 (6H, s, H-3', H-5'), 3.83 (3H, s, OCH<sub>3</sub>-7). ESI-HRMS: *m/z* [M+H]<sup>+</sup> Calcd. 359.1125, found 359.1143.

### 2.3. PL inhibition assay

Stock solutions of the two HPMFs were prepared in DMSO and then various working solutions (20, 40, 60, 80 and 100 μg/mL) were prepared from the stock solution. PL was dissolved in Tris-HCl buffer (50 mM Tris HCl, 150 mM NaCl, 1 mM EDTA, 10 mM MOPS, pH 7.4) and thoroughly mixed for 15–20 min. The final concentration of PL in Tris-HCl buffer was 5 mg/mL [22,23]. This was then incubated with various concentrations of the HPMFs or orlistat (positive control) for 15 min at 37 °C. The total volume of the mixture was kept at 1 mL. Following incubation, 5 μL of PNPB (10 mM in acetonitrile) was added to the mixture and further incubated for 15 min at 37 °C. After 15 min, the absorbance of the mixture was read at 410 nm in a microplate reader (BMG LABTECH SPECTROstar, Germany) against a blank consisting of denatured enzyme. The enzyme mixture was denatured by boiling it at 100 °C for 10 min. Each experiment was repeated three times. The inhibitory activities of HPMFs and orlistat were calculated by measuring the hydrolysis of PNPB to *p*-nitrophenol using the following formula:

$$\text{Inhibition Rate (\% I)} = ((1 - (B - b / A - a)) \times 100$$

where 'A' is the activity of PL without inhibitor and 'a' is the negative control without inhibitor, 'B' is the activity of PL with inhibitor, and 'b' is the negative control with inhibitor [11,24].

### 2.4. Molecular docking and mode of inhibition

To investigate the binding pattern of the HPMFs with PL, molecular docking of HPMFs with porcine PL was performed using the Glide module of the Schrödinger Drug Discovery Platform [25,26]. The 3-dimensional structure of PL (PDB ID: 1LPB) was downloaded from the RCSB Protein Data Bank (<https://www.rcsb.org/>) [27] and used as a template for generating PL ligand-complex models. The structure of the

protein was prepared using the standard protein preparation flow implemented in Schrödinger's Maestro. Crystallographic waters and non-ligand molecules were removed, and incomplete side chains were repaired. Appropriate protonation states were assigned at pH 7.4, and the resulting structure was energy-minimized before docking. The 3D structures of the ligands (HPMFs and the positive control orlistat) were initially constructed in Maestro and prepared for docking using LigPrep. The ligands were then docked into the protein's active site, which was defined by the crystallographic bound ligand, using the induced-fit docking protocol. The protocol was validated by redocking of the cognate ligand (a C11 alkyl phosphonate compound) found in the crystal structure. The protocol could reproduce the crystallographic pose with a RMSD of 1.346 Å, which was well below the 2 Å cut-off typically used in validating docking procedures.

To further confirm the results of the docking study, an *in vitro* study was also performed to determine the mode of inhibition of PL by HPMFs as described by Refs. [22,28]. Briefly, several concentrations of PNPB (20, 40, 60, and 80 μM in acetonitrile) were incubated with PL and HPMFs (100 and 200 μg/mL) for 15 min at 37 °C in Tris-HCl buffer and readings taken every 30 s at 410 nm in a microplate reader (BMG LABTECH SPECTROstar, Germany). A double reciprocal plot (Lineweaver Burk Plot) was used to study the enzyme kinetics, and maximum velocity (V<sub>max</sub>) and Michaelis Menton Constant (K<sub>m</sub>) were calculated by analyzing the double reciprocal plot.

### 2.5. MTT assay

3T3-L1 mouse fibroblast cells were used to investigate the cytotoxicity of HPMFs using the MTT assay following the methodology of [29]; with minor modification. 5 × 10<sup>3</sup> 3T3-L1 cells/well were seeded into 96 wells plates in DMEM supplemented with 1% Pen-Strep and 10% BCS and incubated for 24 h at 37 °C and 5% CO<sub>2</sub>. The media was then removed, and a range of HPMF concentrations were added and the cells further incubated for 72 h. After incubation, the media containing HPMFs was removed, and the cells were washed twice with PBS. Following washing, 100 μL of fresh cell culture media containing 10% freshly prepared MTT solution was added and the cells incubated for a further 4 h, followed by the addition of 100 μL DMSO to dissolve the formazan crystals. After 15 min of incubation with DMSO, the optical absorbance was read at 570 nm in a microplate reader (BMG LABTECH SPECTROstar, Germany). All the assays were done in triplicate and the values were expressed as the percentage of viable cells relative to the control according to the below formula [30]:

$$\% \text{ Viability} = \left( \frac{\text{Mean OD}_{\text{sample}}}{\text{Mean OD}_{\text{blank}}} \right) \times 100$$

### 2.6. 3T3-L1 differentiation

3T3-L1 mouse fibroblast cells were differentiated by following the methodology of [31] with minor modification. The cells were cultured in DMEM supplemented with 10% BCS and 1% Pen-Strep until reaching the contact inhibition stage (3–4 days). The culture media was exchanged for fresh media, and the cells were kept in the post-confluence stage for a further two days. The cells were then induced to differentiate (Day 0: DO) for 3 days in DMEM+10% FBS by using a 3T3-L1 differentiation cocktail which provided a final concentration of 1 μM dexamethasone, 500 μM of 3-isobutyl-1-methylxanthine (IBMX) and 1.5 μg/mL insulin. On day 3 (D3), the differentiation induction media was removed, and the cells were kept in differentiation maintenance media (DMEM + 10% BCS+ 1.5 μg/mL insulin) for 3 days. Various concentrations of HPMFs were also added along with differentiation induction and differentiation maintenance media. The cells were kept in the differentiation maintenance media up to day 10 (D10) (Fig. 1), and the media was exchanged every 2–3 days. Each of the experiment was done in triplicate and all the values were calculated

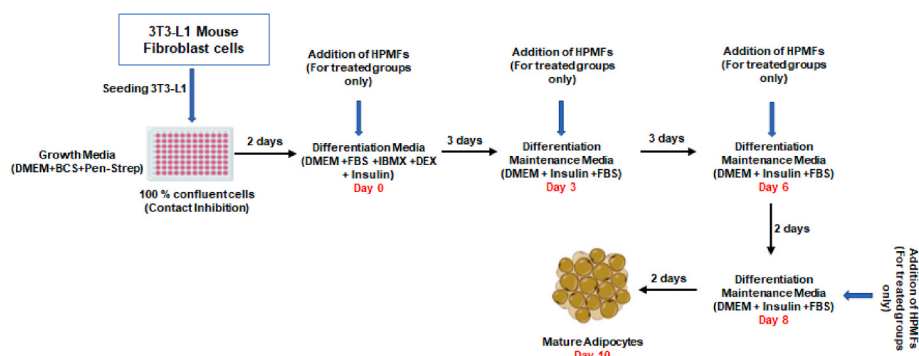


Fig. 1. The differentiation protocol used in this study.

relative to the control (non-treated cells).

## 2.7. Oil Red O staining

To investigate the effects of HPMFs on lipid accumulation, the differentiated adipocytes were stained with Oil red O solution 10 days post-treatment (D10). The staining procedure was performed as described previously [32]. The cells were rinsed with PBS twice and fixed with 10% formaldehyde for 2 h. The cells were then treated with 60% isopropanol solution for 2 min and allowed to dry. Oil red O working solution (0.6% v/v in dH<sub>2</sub>O) was prepared by diluting the stock solution (0.5% w/v in isopropanol) and then 200  $\mu$ L/well was added to the cells. The cells were incubated for 2 h at 37 °C in complete darkness. After 2 h, the Oil Red O working solution was removed and the stained cells were observed and photographed in an inverted fluorescent microscope (Nikon Eclipse, Japan). Oil Red O was quantified by extracting the dye with isopropanol and subsequently reading the absorbance at 490 nm in 96 well dishes in a microplate reader (BMG LATECH SPECTROstar, Germany). The experiments were repeated three times and all the values were calculated as percentage reduction in lipids staining relative to the control (non-treated cells).

## 2.8. Quantification of intracellular triglyceride content

The intracellular triglyceride content of differentiated adipocytes were quantified at 10 days post-treatment (D10) with HPMFs using the triglyceride assay kit (Cat. No. E-BC-K238, USA). The cells were washed with PBS, trypsinized and lysed with RIPA lysis buffer. After lysis, the cells were centrifuged at 13,000 $\times$ g for 20 min and the supernatant was used for the quantification of triglycerides by following the triglyceride assay kit manufacturer's instructions. The samples without treatment of HPMFs were taken as control. The absorbance of the control and treated samples were measured at 510 nm in a microplate reader (BMG LATECH SPECTROstar, Germany). The experiments repeated three times and all the results were expressed as a percentage (%) of triglycerides compared to the control [33].

## 2.9. Glycerol release

The lipolytic effects of HPMFs in 3T3-L1 adipocytes were investigated by incubating the cells for 72 h in the presence and absence of HPMFs, and the release of glycerol (as a result of lipids breakdown) was evaluated. The release of glycerol into the medium was used as an index of lipolysis. Glycerol in the medium was measured according to the instructions of the manufacturer, using a glycerol kit (Catalog No. MAK117, Sigma Aldrich USA). All the values were corrected by subtracting the absorbance of the blank from each sample, and were performed in triplicates. The samples without HPMFs were taken as controls, and all the values were calculated relative to the control.

## 2.10. Gene expression analysis (RT-qPCR)

The effect of HPMFs on the gene expression during the differentiation of 3T3-L1 mouse embryonic fibroblast cells into adipocytes were analyzed through RT-qPCR. The cells were differentiated as described above in the presence and absence of HPMFs. RNA was extracted from both treated and non-treated cells using RNA Extraction Kit (Catalog No. A5001, Promega USA) at D10, and 1  $\mu$ g of total RNA was used to synthesize the first strand of cDNA. The cDNA was synthesized using cDNA Synthesis Kit by Promega, USA (Catalog No. A5001) according to the manufacturer's instruction in a thermocycler (BIO-RAD T100™).

The cDNA was then amplified by using specific sense and antisense primers (0.5  $\mu$ M each) (Table 1) to investigate the expression of adipogenic, cell cycle, lipogenic, and lipolytic genes by RT-qPCR (Eppendorf realplex<sup>2</sup> Master cycler, Germany) using GoTaq™ Master Mix (catalog No. A6001, Promega USA). The samples without HPMFs were taken as control. The experiments were done in triplicate and all the values were normalized to  $\beta$ -actin, which was used as an internal control.

## 2.11. Quantification of protein secretion from adipocytes (adipokines)

The effect of HPMFs on the secretion of adipokines from mature adipocytes was evaluated by following the instructions provided by the

Table 1

List of primer sequences used in this study.

|                                 |                              |
|---------------------------------|------------------------------|
|                                 | 5'-TTCATTCCAACCCACCCCTCCA-3' |
|                                 | 5'-ATGGAGGGGGTCCTTGTTAG-3'   |
| <i>c-Myc</i>                    | 5'-AATCTGCGAGCCAGGACAGG-3'   |
|                                 | 5'-TTCACGTTGAGGGGCATCGT-3'   |
| <i>Cyclin A2</i>                | 5'-TTGGGTTCTTCTCTGGCTCCAA-3' |
|                                 | 5'-GCCTGGAGATGGGAGCGTTA-3'   |
| <i>PPAR<math>\gamma</math></i>  | 5'-GCTTGTGAAGGATGCAAGGGTT-3' |
|                                 | 5'-GCATCCGCCAAAACCTGATG-3'   |
| <i>C/EBP<math>\alpha</math></i> | 5'-ACCAAGTACAATGACCCGCT-3'   |
|                                 | 5'-GCGACCCGAAACCATCTCT-3'    |
| <i>C/EBP<math>\beta</math></i>  | 5'-AGTACAAGATGCGCGCGA-3'     |
|                                 | 5'-CACCTTGCTGCTGCTCCA-3'     |
| <i><math>\alpha</math>P2</i>    | 5'-TCCTCAAACCTGGGCGTGA-3'    |
|                                 | 5'-GCCCGCCATCTAGGGTTAT-3'    |
| <i>FASN</i>                     | 5'-TCCATGGCAGCTGTGGTTTG-3'   |
|                                 | 5'-CAGGCCTCCTGTTCTGACCT-3'   |
| <i>SREBF1</i>                   | 5'-GAAGCTGTCGGGGTAGCGT-3'    |
|                                 | 5'-CCAGCATAGGGGGCGTCAAA-3'   |
| <i>ATGL</i>                     | 5'-GAGCTTCGCGTCACCAACAC-3'   |
|                                 | 5'-CCAGCAGGGCATTCTCTTA-3'    |
| <i>HSL</i>                      | 5'-CTTGGGAGCTCCAGTCGGAA-3'   |
|                                 | 5'-GCGAGTGTACCCAGCGACT-3'    |
| <i>MGL</i>                      | 5'-CGCGCAGTAGTCTGGCTTA-3'    |
|                                 | 5'-GGCAGTCTGGTAGGGAAC-3'     |
| <i><math>\beta</math>-actin</i> | 5'-AGCTCCTCGTTGCCGGTC-3'     |
|                                 | 5'-ATTCCACCACATCACCCCTGG-3'  |

Primer sequences (except Cyclin D1, c-Myc, and Cyclin A2) are taken from [18].

enzyme-linked immunosorbent assay (ELISA) kits manufacturers. To determine adiponectin, leptin and resistin secretion, ELISA kits (Catalog No. E-EL-M0002, E-EL-M3008, E-EL-M3056 respectively) from Elabscience were used. For chemerin, TNF- $\alpha$ , and IL-6, ELISA kits (Catalog No. EM0923, EM0183, EM0121 respectively) from Fine Test China were used. All the reagents were brought to room temperature and freshly prepared each time before use according to the manufacturer's instructions. 100  $\mu$ L of the standard, blank and samples were added to the 96 wells plate and incubated for 90 min at 37  $^{\circ}$ C. After 90 min, the liquid was discarded and, 100  $\mu$ L of biotinylated detection (Ab) working solution was immediately added and the plate incubated for 1 h at 37  $^{\circ}$ C. The liquid was then aspirated, and the plate was washed three times with distilled water and dried. After this, 100  $\mu$ L of HRP conjugate working solution was added and the plate incubated for 30 min at 37  $^{\circ}$ C. The liquid was then aspirated, and the plate was washed five times again with distilled water. Then 100  $\mu$ L of substrate reagent was added and incubated at 37  $^{\circ}$ C for 15 min, followed by adding 50  $\mu$ L of stop solution. Each experiment was done in duplicate and the absorbance was measured at 450 nm in an ELISA microplate reader (BMG LATECH SPECTROstar, Germany).

### 2.12. Statistical analysis

GraphPad Prism statistical software (version 8.0) was used for statistical analysis. All the data are expressed as mean  $\pm$  standard deviations. A one-way and two-way analysis of variance (ANOVA) followed by the Tukey test was used for statistical analysis. Statistical significance of the data is denoted as \* $p$  < 0.05, \*\* $p$  < 0.01, \*\*\* $p$  < 0.001, and \*\*\*\* $p$  < 0.0001.

## 3. Results

### 3.1. Synthesis of HPMFs

The two hydroxy-polymethoxyflavones (HPMFs) used in this study

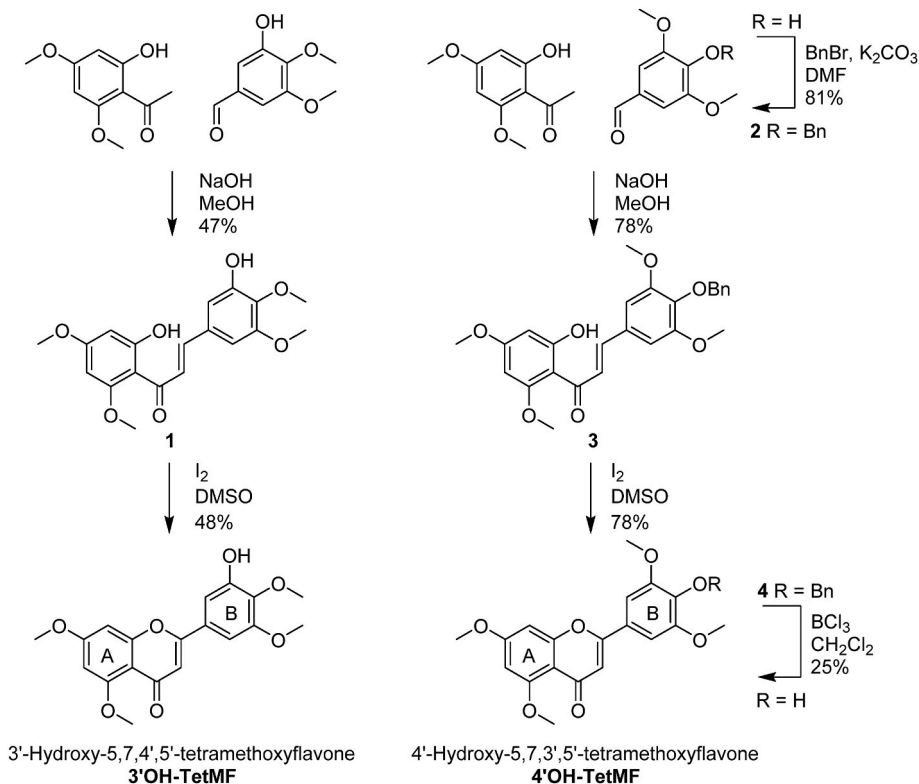
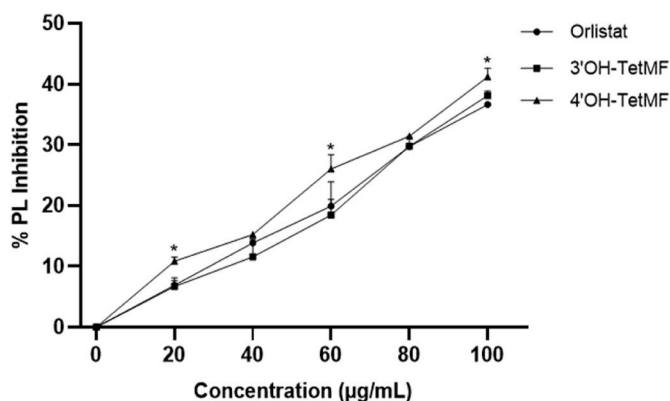


Fig. 2. Synthesis of the HPMFs used in this study. Assignment of A and B rings indicated on the products.

were synthesized by iodine-catalysed oxidative ring closure of the corresponding chalcones (Fig. 2) [34]. The chalcones were in turn prepared by crossed aldol (Claisen-Schmidt) reactions [35] from suitably substituted aromatic ketones (for the A-ring) and aromatic aldehydes (B ring). In the case of 3'-hydroxy-5,7,4',5'-tetramethoxyflavone (3'OH-TetMF) this was achieved directly in two steps via compound 1. However, for 4'-hydroxy-5,7,3',5'-tetramethoxyflavone (4'OH-TetMF), as suggesting in the literature [36], it was found that the cyclisation reaction did not proceed cleanly, and a protecting group strategy was used. A benzyl group was appended to the free alcohol in the aldehyde precursor to give 2 [37], and after aldol yielding 3 and oxidative ring closure to achieve 4, the protecting group was removed using boron trichloride [38]. All products were purified by automated column chromatography and isolated as pure off-white solids.

### 3.2. HPMFs reduce PL activity

The inhibitory effects of the two HPMFs on porcine PL were investigated using a range of concentrations (20, 40, 60, 80, and 100  $\mu$ g/mL). Both of the HPMFs inhibited the activity of PL in a concentration-dependent manner. 4'OH-TetMF inhibited PL activity by 10, 15, 26, 31 and 41% while 3'OH-TetMF inhibited PL by 7, 11, 18, 30 and 37% at 20, 40, 60, 80, and 100  $\mu$ g/mL of each HPMF respectively (Fig. 3). Orlistat was used as a positive control and inhibited the activity of PL by 36% at the highest concentration (100  $\mu$ g/mL). The PL inhibitory effects of 4'OH-TetMF at 40, 60 and 100  $\mu$ g/mL were significantly higher than 3'OH-TetMF, while at 20 and 80  $\mu$ g/mL, the PL inhibitory effects of 4'OH-TetMF and 3'OH-TetMF were almost same. Moreover, the PL inhibitory effects of 4'OH-TetMF at 40, 60 and 100  $\mu$ g/mL were also significantly higher than the positive control orlistat. There were no significant differences between the inhibitory effects of 3'OH-TetMF and orlistat at any concentration (20–100  $\mu$ g/mL).



**Fig. 3.** Inhibitory effects of 3'OH-TetMF and 4'OH-TetMF on the activity of PL. Asterisks represent significant differences ( $p < 0.05$ ) of PL inhibitory effects of 4'OH-TetMF from 3'OH-TetMF and orlistat at 20, 60 and 100 µg/mL. No significant difference was observed between 3'OH-TetMF and orlistat. This graph is representative of three independent experiments.

### 3.3. Molecular docking and mode of inhibition

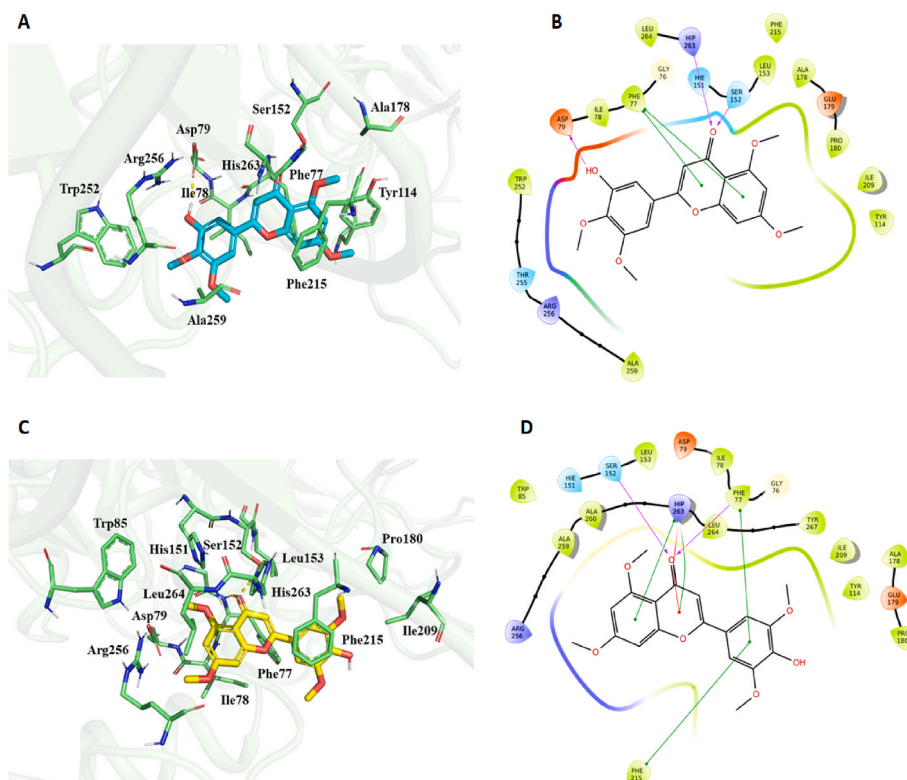
To understand the binding pattern and affinity of each HPMF with PL, molecular docking was performed on porcine PL using an induced-fit docking protocol [39]. Both of the HPMFs interacted with residues within the PL active site (Fig. 4). Crystal structures of PL have shown that it is constituted by two structural domains, a N-terminal domain which comprised of amino acid residues 1–336, and a C-terminal domain which contains amino acid residues 336–449 [40–42]. The N-terminal domain functions as the catalytic domain and contains the catalytic triad (Ser152-His263-Asp176) which is shielded by the lid domain. Meanwhile, the C-terminal domain is involved in colipase

binding [40] and is crucial for non-catalytic functions such as binding of lipids, heparin and cofactors [41]. Conformational changes in PL occurs during which the lid is opened and exposes the hydrophobic part of the active site which enhances the binding capacity of the substrate with the catalytic site of PL [43].

Our docking results indicated that the binding affinity of 4'OH-TetMF with PL was stronger (−9.12 kcal/mol) than 3'OH-TetMF (−8.39 kcal/mol) and orlistat (−8.05 kcal/mol). 3'OH-TetMF was found to form three hydrogen bonds to known key residues in the PL binding site such as Ser152, His263, and Asp79 and was additionally stabilized by  $\pi$ - $\pi$  stacking interactions with Phe77. On the other hand, 4'OH-TetMF adopted a slightly different binding pose and was found to form two hydrogen bonds with Phe77 and Ser152. Despite the fewer hydrogen bond interactions, we observed an additional  $\pi$ -cation interaction between 4'OH-TetMF and His263, as well as numerous  $\pi$ - $\pi$  stacking interactions with Phe77, Phe215, and His263. These additional interactions potentially explain the favourable predicted binding energy of 4'OH-TetMF. Our docking results were therefore in agreement with our *in vitro* PL inhibition results, whereby 4'OH-TetMF which had the best docking score also showed greater PL inhibition compared to 3'OH-TetMF and the positive control orlistat, which had similar docking scores and PL inhibition. This further lent credence to the binding poses of both HPMFs observed here, which showed that they may inhibit the activity of PL in a competitive manner. The mode of inhibition of PL by HPMFs was therefore further investigated using the PL assay to generate a Lineweaver Burk Plot, and  $V_{max}$  and  $K_m$  values were determined (Table 2). Consistent with the molecular docking results, both HPMFs inhibited PL activity in a competitive manner (Fig. 5).

### 3.4. Cytotoxicity of HPMFs (MTT assay)

To investigate the cytotoxic effects of 3'OH-TetMF and 4'OH-TetMF, 3T3-L1 mouse fibroblast cells were seeded (24hrs) followed by

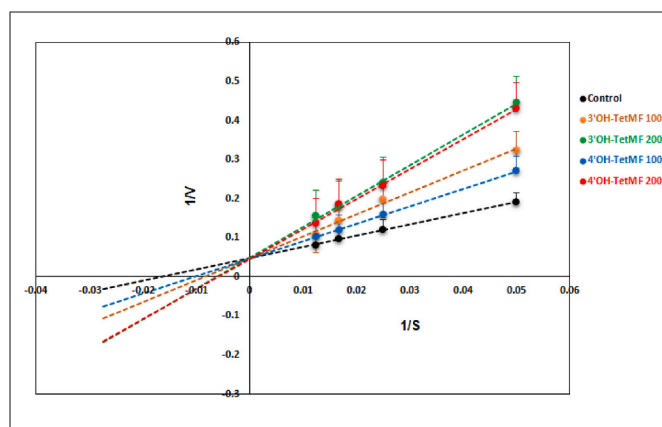


**Fig. 4.** 3D models (A and C) of key binding interactions and 2D ligand interaction diagrams (B and D) of 3'OH-TetMF (A and B) and 4'OH-TetMF (C and D) docked to porcine PL (PDB: 1LPB). Hydrogen bonds are shown as yellow dashed lines (A and C), or as purple arrows (B and D).  $\pi$ - $\pi$  stacking interactions are shown as green lines, while cation- $\pi$  interactions are shown as red lines (B and D).

**Table 2**

Kinetic parameters of PL activity in the presence and absence of inhibitors (HPMFs).

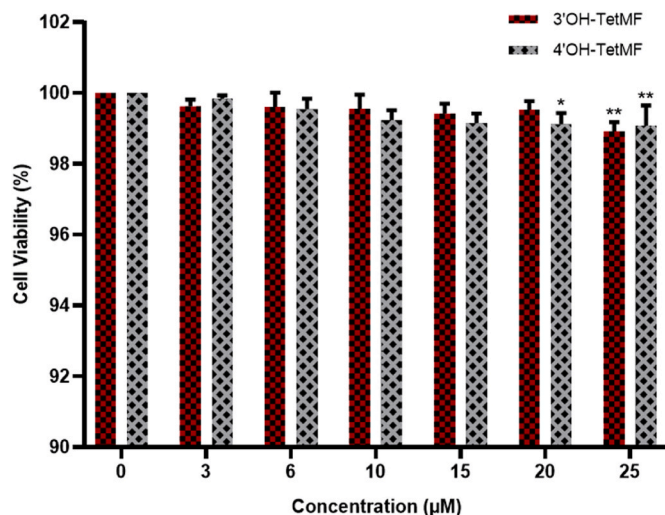
|   | Velocity ( $\mu\text{M}/\text{min}$ ) of Enzyme Activity at different substrate concentrations ( $\mu\text{M}$ ) |                 |                 |                 | Vmax ( $\mu\text{M}/\text{min}$ ) | Km ( $\mu\text{M}$ ) |
|---|--|-----------------|-----------------|-----------------|-----------------------------------|----------------------|
|   | 20   | 40              | 60              | 80              |                                   |                      |
| <b>Control</b>  | 5.2 $\pm$ 0.26   | 8.2 $\pm$ 0.27  | 15.1 $\pm$ 0.19 | 12.3 $\pm$ 0.05 | 20.83                             | 60.01                |
| <b>Concentration (<math>\mu\text{g}/\text{mL}</math>)</b> |  |                 |                 |                 |                                   |                      |
| <b>3'OH-TetMF (100)</b>                                   | 3.08 $\pm$ 0.03  | 5.06 $\pm$ 0.1  | 6.98 $\pm$ 0.13 | 9.14 $\pm$ 0.21 | 20.92                             | 110.10               |
| <b>3'OH-TetMF (200)</b>                                   | 2.23 $\pm$ 0.06  | 4.16 $\pm$ 0.03 | 5.56 $\pm$ 0.02 | 6.46 $\pm$ 0.07 | 20.08                             | 155.44               |
| <b>4'OH-TetMF (100)</b>                                   | 3.69 $\pm$ 0.05  | 6.24 $\pm$ 0.03 | 8.31 $\pm$ 0.01 | 9.6 $\pm$ 0.01  | 21.00                             | 93.62                |
| <b>4'OH-TetMF (200)</b>                                   | 2.32 $\pm$ 0.03  | 4.27 $\pm$ 0.05 | 5.4 $\pm$ 0.02  | 7.3 $\pm$ 0.03  | 21.27                             | 163.17               |

**Fig. 5.** Kinetic analysis (Lineweaver Burk Plot) of PL assays performed in the presence and absence of 100 and 200  $\mu\text{g}/\text{mL}$  of 3'OH-TetMF or 4'OH-TetMF. Each experiment was repeated three times.

incubation with various concentrations (0, 3, 6, 10, 15, 20 and 25  $\mu\text{M}$ ) of HPMFs for 72 h, after which the MTT assay was performed. 3'OH-TetMF showed a small but statistically significant effect in this assay at 25  $\mu\text{M}$  while 4'OH-TetMF showed a small but significant effect at 20  $\mu\text{M}$  relative to the control (Fig. 6). Both HPMFs had no effect on 3T3-L1 cells in this assay, up to 15  $\mu\text{M}$ , relative to the control. Therefore, 15  $\mu\text{M}$  was the highest concentration used for further assays.

### 3.5. HPMFs inhibit lipid accumulation during adipogenesis

The inhibitory effect of 3'OH-TetMF and 4'OH-TetMF on the accumulation of lipids was investigated during 3T3-L1 mouse fibroblast cell differentiation into mature adipocytes. The cells were induced to differentiate using a cocktail of 1  $\mu\text{M}$  dexamethasone, 500  $\mu\text{M}$  of IBMX and 1.5  $\mu\text{g}/\text{mL}$  insulin as described in the materials and methods and shown in Fig. 1, and incubated with various concentrations (0, 3, 6, 10, 15  $\mu\text{M}$ ) of 3'OH-TetMF or 4'OH-TetMF until D10. Both of the HPMFs significantly reduced the accumulation of lipids during the differentiation of preadipocytes to mature adipocytes (Figs. 7 and 8). The overall effect of 4'OH-TetMF on lipid accumulation was greater than for 3'OH-TetMF. 3'OH-TetMF reduced lipid accumulation by 10, 17, 36, and 47%, while 4'OH-TetMF reduced the lipid accumulation by 12, 30, 46, and 58% at 3, 6, 10 and 15  $\mu\text{M}$  of each HPMF respectively.

**Fig. 6.** Cytotoxic effects of 3'OH-TetMF and 4'OH-TetMF in 3T3-L1 cells at the concentrations indicated. Data is represented as mean  $\pm$  SD ( $n = 3$  biological repeats), and  $p < 0.05$  was considered as significantly different. \* $p < 0.05$ , \*\* $p < 0.01$ .

### 3.6. HPMFs inhibit triglyceride accumulation

The inhibitory effects of 3'OH-TetMF and 4'OH-TetMF on the accumulation of triglycerides were investigated at day 10 (D10) after treatment with each HPMF during 3T3-L1 mouse fibroblast cell differentiation into adipocytes. Both of the HPMFs significantly reduced the accumulation of triglycerides in a dose-dependent manner relative to the control cells (Fig. 9). 3'OH-TetMF reduced the accumulation of triglycerides by 8, 17, 24, and 38% at 3, 6, 10 and 15  $\mu\text{M}$  respectively. Furthermore, 4'OH-TetMF, significantly reduced triglyceride accumulation by 11, 20, 32, and 39% at 3, 6, 10 and 15  $\mu\text{M}$  respectively. The cells without any treatment with HPMFs were considered as 100% mature adipocytes, and the triglyceride content of these non-treated adipocytes was normalized to 100%. Each experiment was repeated three times and all the values were expressed in terms of percentage relative to the non-treated cells (0  $\mu\text{M}$ ).

### 3.7. HPMFs enhance glycerol release from mature adipocytes

The effects of HPMFs on the release of glycerol from mature adipocytes were investigated at D10. The cells were treated with either 3, 6, 10 or 15  $\mu\text{M}$  of 3'OH-TetMF or 4'OH-TetMF for 72 h. After 72 h, the release of glycerol into the culture medium was measured. Both HPMFs significantly enhanced the release of glycerol from mature adipocytes (Fig. 10), indicating that they can accelerate lipid breakdown in mature adipocytes. The release of glycerol from non-treated mature adipocytes was taken as 100%, while glycerol release from the treated adipocytes was calculated as relative to the non-treated (control) adipocytes. There was no significant difference between the effect of 3'OH-TetMF and 4'OH-TetMF at 3 and 6  $\mu\text{M}$  of each compound. 3'OH-TetMF increased the release of glycerol to 117 and 131%, while 4'OH-TetMF enhanced glycerol release to 117 and 132% at 3 and 6  $\mu\text{M}$  of each compound respectively. At 10 and 15  $\mu\text{M}$ , the effect of 4'OH-TetMF was higher than 3'OH-TetMF. 4'OH-TetMF enhanced glycerol release to 166 and 192% while 3'OH-TetMF enhanced glycerol release to 154 and 168% at the same concentrations.

### 3.8. HPMFs inhibit adipogenic and lipogenic genes expression

The effects of 3'OH-TetMF and 4'OH-TetMF on the expression of adipogenic and lipogenic genes were investigated during the differentiation and incubation of 3T3-L1 cells with and without HPMFs as

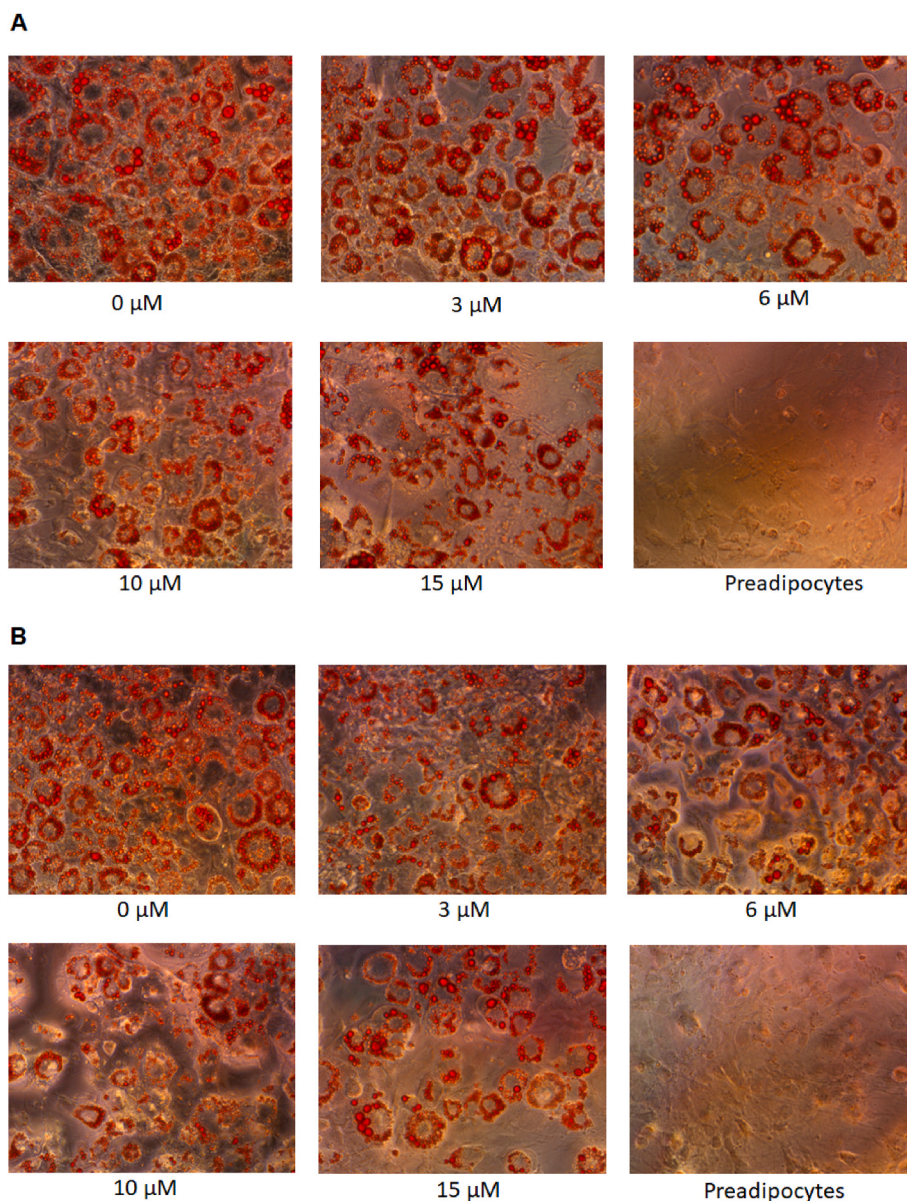
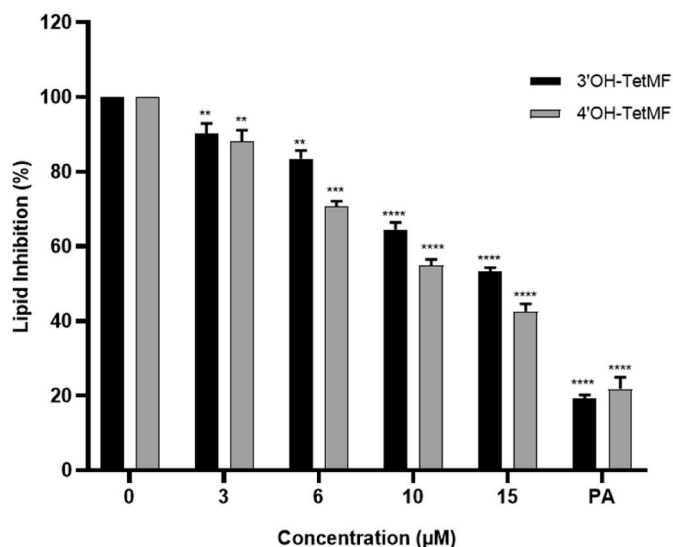


Fig. 7. Oil Red O staining at day 10 (D10), after treatment with either (A) 3'OH-TetMF or (B) 4'OH-TetMF at the indicated concentrations during 3T3-L1 mouse fibroblast cell differentiation into adipocytes.

described in the methodology. Both of the HPMFs significantly reduced the expression of mRNA of adipogenic and lipogenic genes at 10 and 15 μM of each HPMF (Fig. 11). The expression of genes in the control (0 μM) was considered 100%. The values of the expression of genes in the treated samples were expressed in terms of percentage relative to the control sample. β-actin was used as an internal control. 3'OH-TetMF reduced the expression of PPAR $\gamma$ , C/EBP $\alpha$ , C/EBP $\beta$ , aP2, SREBF1 and FASN by 26 and 53%, 48 and 49%, 42 and 76%, 52 and 59%, 42 and 49%, 50 and 79%, at 10 and 15 μM respectively (Fig. 11 A, C, E, G, I, and K). Likewise, 4'OH-TetMF reduced the expression of PPAR $\gamma$ , C/EBP $\alpha$ , C/EBP $\beta$ , aP2, SREBF1 and FASN by 49 and 81%, 42 and 50%, 53 and 82%, 60 and 72%, 70 and 82%, and 67 and 70% at 10 and 15 μM of compound respectively (Fig. 11 B, D, F, H, J, and L). Overall, the effects of 4'OH-TetMF were greater than with 3'OH-TetMF, which is consistent with earlier results obtained in the case of lipid accumulation (oil red o staining), and quantification of triglyceride accumulation and glycerol release.

### 3.9. HPMFs regulate cell cycle gene expression during adipogenesis

To investigate whether 3'OH-TetMF and 4'OH-TetMF have any effect on the regulation of cell cycle genes that encode C-Myc, Cyclin D1 and Cyclin A2, after induction of differentiation, the cells were incubated with 10 and 15 μM HPMFs for 72 h. Both of the HPMFs significantly enhanced the expression of C-Myc and Cyclin D1 and decreased the expression of Cyclin A2 (Fig. 12). The expression of genes in the control sample was taken as 1 (100% expression), while in all other treated samples, their expression was calculated as relative to the control sample. 3'OH-TetMF increased the expression of C-Myc by 1.48 and 2.27 fold (Fig. 12 A) while 4'OH-TetMF enhanced its expression by 1.3 and 2.5 fold at 10 and 15 μM respectively (Fig. 12B). Likewise, the expression of Cyclin D1 was increased by 1.71 and 1.97 fold upon treatment with 10 and 15 μM of 3'OH-TetMF respectively, while its expression was increased by 3.18 and 3.48 fold upon treatment with 4'OH-TetMF at the same concentrations respectively. On the other hand, the expression of cyclin A2 was reduced by 0.1 and 0.28 fold when treated with 3'OH-TetMF (10 and 15 μM) and by 0.33 and 0.51 upon



**Fig. 8.** Quantification of Oil Red O staining at day 10 (D10), after treatment with either 3'OH-TetMF or 4'OH-TetMF at the indicated concentrations during 3T3-L1 mouse fibroblast cell differentiation into adipocytes. Each value is expressed as mean  $\pm$  S.D. (n = 3). Different asterisks show significant differences ( $p < 0.05$ ) from control (0  $\mu$ M). \*\* $p < 0.01$ , \*\*\* $p < 0.001$ , \*\*\*\* $p < 0.0001$ . PA: Preadipocytes (non-differentiated 3T3-L1 mouse fibroblast cells).

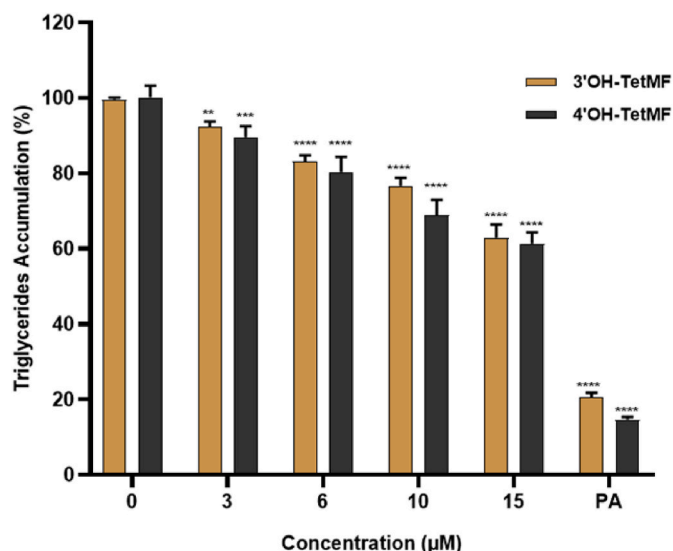


**Fig. 9.** Effects of 3'OH-TetMF and 4'OH-TetMF at the indicated concentrations during 3T3-L1 mouse fibroblast cell differentiation into adipocytes on the accumulation of triglycerides at day 10 (D10). Each value is expressed as mean  $\pm$  S.D. (n = 3). A Two way ANOVA followed by Tukey test was used to determine the significant differences ( $p < 0.05$ ). \*\* $P < 0.01$ , \*\*\* $p < 0.001$ , \*\*\*\* $p < 0.0001$ .

treatment with 10 and 15  $\mu$ M of 4'OH-TetMF respectively.

### 3.10. HPMFs enhance lipolytic genes expression during differentiation

3T3-L1 cells were seeded at  $1.5 \times 10^4$  cells/well in 24 well plates and induced to differentiate in the presence and absence of 3'OH-TetMF and 4'OH-TetMF and the expression of lipolysis related genes (ATGL, HSL, MGL) were investigated at day 10 (D10). The expression of genes was determined by fold-change in expression relative to the control sample (Fig. 13). The lipolytic gene expression in the control sample was taken as 1, and all values were normalized to  $\beta$ -actin. 3'OH-TetMF increased

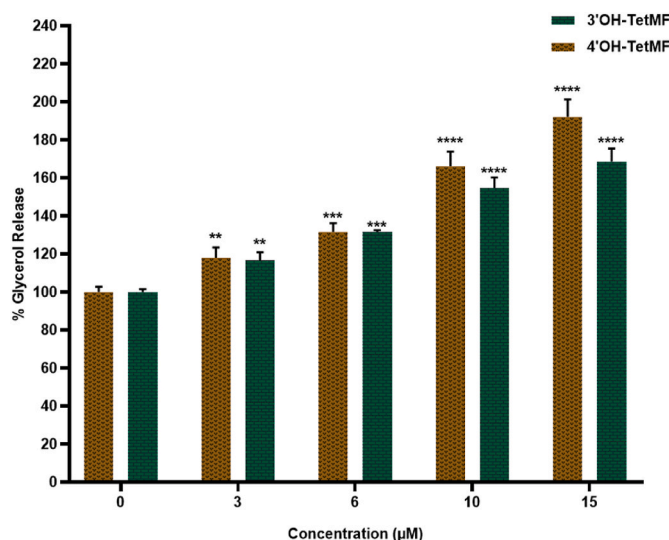


**Fig. 10.** Effects of 3'OH-TetMF and 4'OH-TetMF on the release of glycerol from 3T3-L1 adipocytes, 10 days post-treatment (D10). Two-way ANOVA followed by Tukey test was used to determine the significant differences ( $p < 0.05$ ). Each experiment was done in triplicate. \*\* $p < 0.01$ , \*\*\* $p < 0.001$ , \*\*\*\* $p < 0.0001$ .

the gene expression of ATGL, HSL, and MGL by 1.46 and 1.58, 2.69 and 2.63, 2.7 and 3.6 fold at 10 and 15  $\mu$ M concentrations. Similarly, 4'OH-TetMF enhanced ATGL, HSL, and MGL expression by 2.0 and 3.3, 3.2 and 3.7, and 1.37 and 1.94 fold at the same concentrations.

### 3.11. Effects of HPMFs on secretable proteins (adipokines)

#### 3.11.1. TNF- $\alpha$ and IL-6 secretion (pro-inflammatory cytokines)

3T3-L1 cells were differentiated in the presence and absence of HPMFs as described in the methodology and the effects of 3'OH-TetMF and 4'OH-TetMF on the secretion of pro-inflammatory cytokines (TNF- $\alpha$  and IL-6) were investigated at D10 (Fig. 14). The secretion of TNF- $\alpha$  and IL-6 in the control samples were considered as 100% and all the values were expressed in terms of percentage (%) relative to the control. 3'OH-TetMF reduced TNF- $\alpha$  secretion by 10, 14 and 20% at 6, 10 and 15  $\mu$ M respectively, while at 3  $\mu$ M, it did not show a significant effect as compared to the untreated control sample (100%). Similarly, 3'OH-TetMF reduced IL-6 secretion significantly by 10, 23 and 29% at 6, 10 and 15  $\mu$ M respectively, while at 3  $\mu$ M, it did not have significant effect on IL-6 secretion versus the untreated control sample. 4'OH-TetMF also significantly reduced the secretion of TNF- $\alpha$  by 11, 19 and 25% at 6, 10 and 15  $\mu$ M respectively versus the untreated control. In the case of IL-6, 4'OH-TetMF decreased its secretion to 5, 7, 16 and 26% at 3, 6, 10 and 15  $\mu$ M respectively.

#### 3.11.2. Resistin and chemerin secretion

The effect of 3'OH-TetMF and 4'OH-TetMF on the secretion of resistin and chemerin was investigated in mature adipocytes after differentiating the cells until D10 in the presence and absence of HPMFs (Fig. 15). The secretion of chemerin and resistin from the control samples were considered as 100% and all the values were expressed in terms of percentage (%) relative to the control. 3'OH-TetMF and 4'OH-TetMF did not significantly affect the secretion of resistin at 3  $\mu$ M relative to the control (Fig. 15). 3'OH-TetMF reduced resistin secretion significantly by 8, 17 and 23%, while 4'OH-TetMF reduced resistin secretion significantly by 8, 13, and 20% at the 6, 10 and 15  $\mu$ M respectively (Fig. 15 A). In the case of chemerin secretion, 3'OH-TetMF reduced chemerin secretion significantly by 21 and 33% only at 10 and 15  $\mu$ M respectively, while at 3 and 6  $\mu$ M, it did not have any significant effect on chemerin secretion. 4'OH-TetMF did not significantly affect chemerin

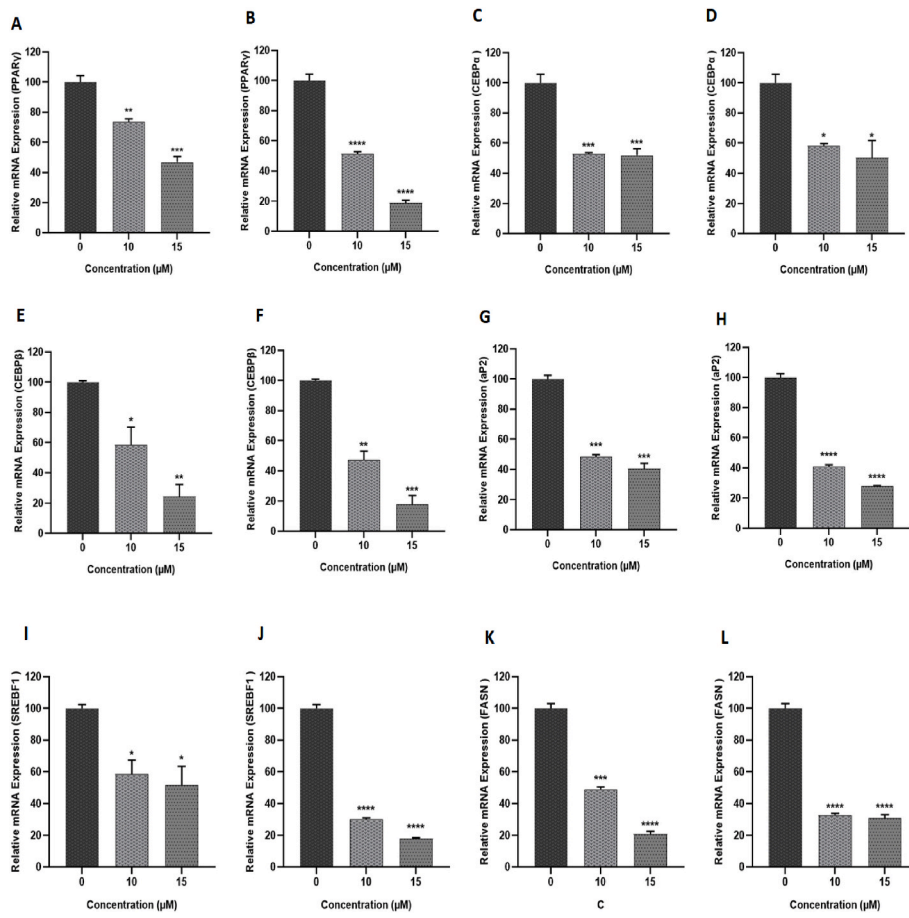


**Fig. 11.** Effects of 3'OH-TetMF and 4'OH-TetMF on the expression of positive marker genes of adipogenesis and lipogenesis during the differentiation 3T3-L1 cells into mature adipocytes. A, C, E, G, I, and K show the expression of genes when treated with 3'OH-TetMF on D0 at the indicated concentrations and analysis performed on D10. B, D, F, H, J, and L show the expression of genes after treatment with 4'OH-TetMF on D0 at the concentrations indicated and analysis performed on D10. Each value is expressed as mean ± S.D. (n = 3). One-way ANOVA with Tukey test was used to determine the significant differences (p < 0.05). β actin was used as an internal control. \*p < 0.05, \*\*p < 0.01, \*\*\*p < 0.001, \*\*\*\*p < 0.0001.

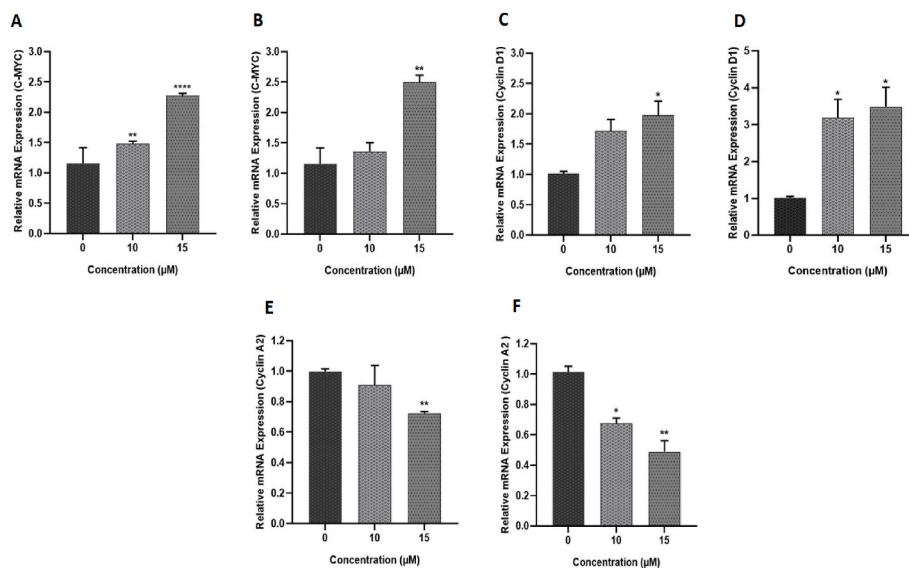


**Fig. 12.** Effects of 3'OH-TetMF and 4'OH-TetMF on the expression of cell cycle genes in 3T3-L1 adipocytes, 72 h post-treatment. A, C, E show the expression of gene when treated with 3'OH-TetMF, while B, D, F, H, J, and L show the expression of genes after treatment with 4'OH-TetMF at the indicated concentrations, 72 h post-treatment. All the values are normalized to β actin which was used as an internal control. Each value is expressed as mean ± S.D. (n = 3). One way ANOVA with Tukey test was used to determine the significant differences (p < 0.05). \*p < 0.05, \*\*p < 0.01, \*\*\*p < 0.001, \*\*\*\*p < 0.0001.

secretion at 3 μM, while 6, 10, and 15 μM, significantly reduced chemerin secretion by 12, 28, and 34% respectively (Fig. 15 B).

**3.11.3. Adiponectin and leptin secretion**

The effect of 3'OH-TetMF and 4'OH-TetMF on the secretion of adiponectin and leptin proteins from adipocytes was investigated 10 days after induction of adipocytes differentiation in the presence and absence of HPMFs (Fig. 16). In the case of adiponectin, 3'OH-TetMF, did

not have any significant effect at 3 μM, while at 6, 10 and 15 μM it enhanced the secretion of adiponectin significantly by 17, 49 and 56%, as compared to the untreated control sample. Likewise, 4'OH-TetMF also showed the same pattern, but its effect was slightly greater than with 3'OH-TetMF. At 6, 10 and 15 μM it enhanced adiponectin secretion by 21, 55 and 73% (Fig. 16 A). The secretion of leptin is opposite to that of adiponectin. In obesogenic conditions, its secretion is increased, and tightly correlated with the expansion of adipocytes [44,45]. In the

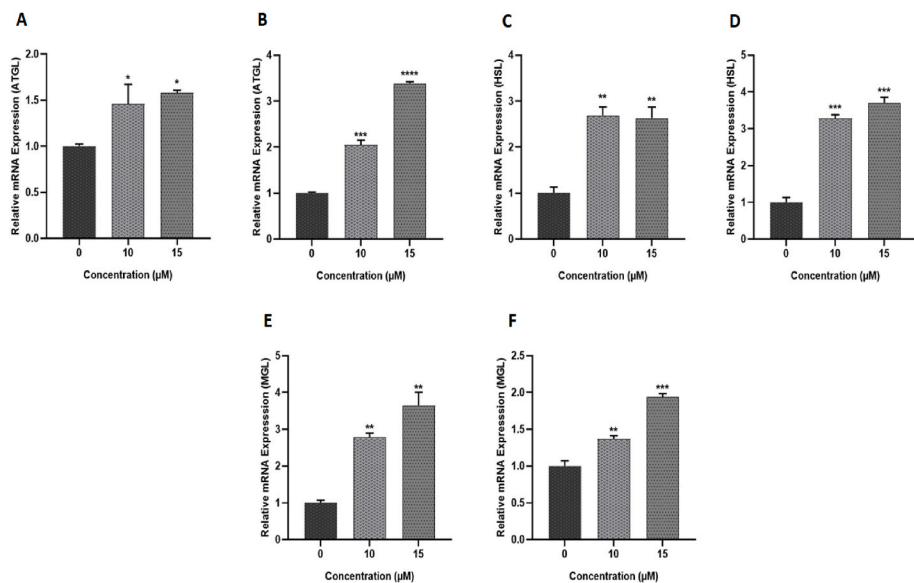


**Fig. 13.** Effects of 3'OH-TetMF and 4'OH-TetMF on lipolysis-related genes expression during differentiation of 3T3-L1 cells into adipocytes. A, C, E shows the genes expression of ATGL, HSL, and MGL after treating the cells with 3'OH-TetMF, while B, D, and F show the genes expression after treatment with 4'OH-TetMF on D0 at the concentrations indicated and analysis performed on D10.  $\beta$  actin was used as an internal control. The experiment was done in triplicate, and each value is expressed as mean  $\pm$  S.D. (n = 3). One way ANOVA with Tukey test was used to determine the significant differences ( $p < 0.05$ ). \* $p < 0.05$ , \*\* $p < 0.01$ , \*\*\* $p < 0.001$ , \*\*\*\* $p < 0.0001$ .

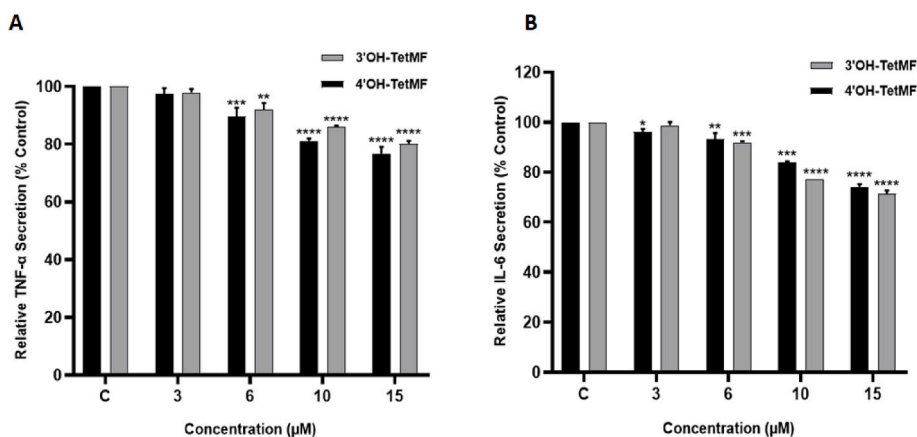


**Fig. 14.** Effects of 3'OH-TetMF and 4'OH-TetMF on (A) TNF- $\alpha$  and (B) IL-6 secretion. The experiments were done in duplicates, and each value is expressed as mean  $\pm$  S.D. (n = 2). Significance was calculated for each HTMF versus an untreated control. \* $p < 0.05$ , \*\* $p < 0.01$ , \*\*\* $p < 0.001$ , \*\*\*\* $p < 0.0001$ .

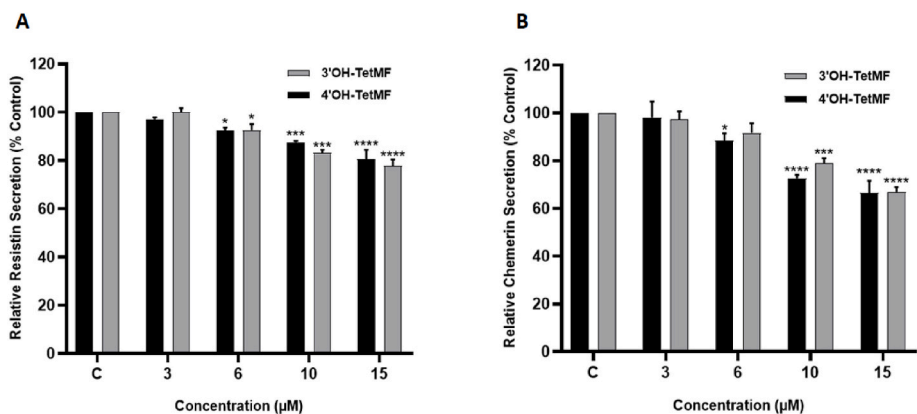


**Fig. 15.** Effects of 3'OH-TetMF and 4'OH-TetMF on (A) resistin and (B) chemerin secretion. The experiments were done in duplicates, and each value is expressed as mean  $\pm$  S.D. (n = 2). Significance was calculated for each compound versus an untreated control \* $p < 0.05$ , \*\* $p < 0.01$ , \*\*\* $p < 0.001$ , \*\*\*\* $p < 0.0001$ .

current study, both HPMFs significantly reduced the secretion of leptin from adipocytes (Fig. 16 B). Its secretion was reduced by 16, 46 and 64% upon treatment with 6, 10, and 15  $\mu$ M of 3'OH-TetMF, while at 3  $\mu$ M it did not have significant effect on the secretion of leptin. Likewise,

leptin's secretion was reduced significantly by 11, 29, 60 and 69% at 3, 6, 10, and 15  $\mu$ M of 4'OH-TetMF (Fig. 16 B).

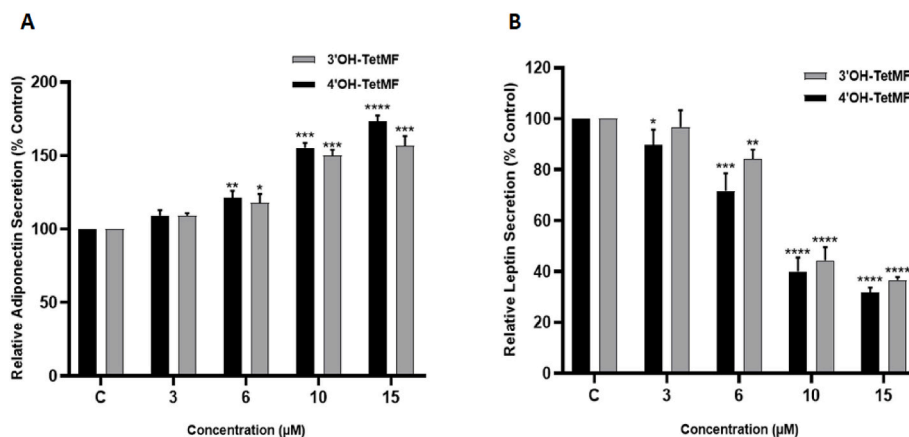


**Fig. 16.** Effect of 3'OH-TetMF and 4'OH-TetMF on (A) adiponectin and (B) leptin secretion. The experiments were done in duplicates, and each value is expressed as mean  $\pm$  S.D. (n = 2). Significance was calculated for each HTMF versus an untreated control. \*p < 0.05, \*\*p < 0.01, \*\*\*p < 0.001, \*\*\*\*p < 0.0001.

#### 4. Discussion

Obesity is one of the major health threats in the 21st century due to its contribution to the prevalence of other health comorbidities [46]. Previously, HPMFs have been shown to exhibit anti-obesity properties [47–50], with their efficacies dependent on the distribution of hydroxy (-OH) and methoxy (-OCH<sub>3</sub>) groups on A and B rings of the basic flavone skeleton [19]. Two new HPMFs, 3'OH-TetMF and 4'OH-TetMF (Fig. 2), are used in this study to investigate their effects against obesity. Of the two flavones used in this study, 3'OH-TetMF is found in nature also. It has been observed to occur as a result of biotransformation when plants were fed non-natural starting materials [51] and has been found in the leaves of *Murraya paniculate* also [52]. The anti-obesity effects of the two HPMFs were quite similar, although overall, the effects of 4'OH-TetMF were greater than those seen with 3'OH-TetMF. In the case of PL inhibition, 4'OH-TetMF effects were significantly higher versus 3'OH-TetMF and the positive control orlistat (Fig. 3). This was also evident from the binding efficacies of the HPMFs with PL in molecular docking. This revealed that these HPMFs bind to residues Ser152 and His263 of the active site of PL and hence can show competitive inhibition (Fig. 4). In competitive inhibition, the inhibitors bind to the active site of protein [53,54]. This finding was supported by the *in vitro* enzyme kinetics study, which also demonstrated competitive inhibition of PL by both HPMFs (Fig. 5). In competitive inhibition, the Km values increases while the maximum reaction rate (Vmax) remains unchanged [55]. In this study, the Vmax values of the two HPMFs did not change significantly while the Km values increased with the increase concentration of HPMFs (Table 2) which also indicated competitive inhibition of PL by these HPMFs.

In molecular docking, a lower binding energy indicates a more stable interaction of the ligand with the receptor [56,57]. The binding energies of the HPMFs used in this study were found to be in agreement with their PL inhibition *in vitro*. The binding energy of 4'OH-TetMF was -9.12 kcal/mol, 3'OH-TetMF was -8.39 kcal/mol, and the positive control orlistat was -8.05 kcal/mol which indicates stronger interaction pattern of 4'OH-TetMF than 3'OH-TetMF and orlistat. The better binding energy observed in the case of 4'OH-TetMF might be due to the presence of a hydrophobic -OCH<sub>3</sub> group at position 3' of the B ring. The position and number of -OH and -OCH<sub>3</sub> groups on B ring of flavones also greatly influences their metabolism and hence their efficacies [58]. So, the presence of the -OCH<sub>3</sub> group at position 3' of the B ring may have improved the binding of 4'OH-TetMF with PL, hence exerting a greater inhibition on PL. Huang et al. [59] also reported similar higher inhibitory effects of the flavones which possessed a -OCH<sub>3</sub> group at position 3' of the B ring on the flavone skeleton. Nobiletin (5,6,7,8,3',4'-hexamethoxyflavone) and 5-demethylnobiletin (5-hydroxy-3',4',6,7,

8-pentamethoxyflavone) showed higher inhibitory activity than tangeretin (4',5,6,7,8-pentamethoxyflavone) and 5-demethyltangeretin (5-hydroxy 4',6,7,8-tetramethoxyflavone) [59]. In this regard, the results obtained in our study were consistent with those reported by Huang et al. [59]. This also indicates that hydroxylation at position 4' of B ring might be more important for the inhibition of PL activity.

Previously, some flavones have been reported to exhibit mixed mode inhibition against PL. In particular, [59] reported that nobiletin, 5-demethylnobiletin, tangeretin and 5-demethyltangeretin exhibit mixed mode inhibition against PL. In this case, the results of our study were inconsistent with those of [59]; in that we observed competitive inhibition only. Conversely Liang et al. [56], reported that apigenin (a trihydroxyflavone) exhibits a competitive mode of inhibition against PL. This indicates that although flavones belong to the same molecular class (flavonoids) and are potent inhibitors of PL, their mode of inhibition may vary according to the number, type and positions of side chains attached to the basic flavone skeleton.

In cell studies, it was observed that these HPMFs possess anti-adipogenic effects and significantly suppress the development of pre-adipocytes to mature adipocytes. As expected, in cell studies, the overall anti-obesity effects of 4'OH-TetMF were higher than with 3'OH-TetMF. Both HPMFs significantly reduced lipid and triglyceride accumulation (Figs. 7–9) during preadipocyte differentiation, as evidenced by Oil Red O staining. Similar results were obtained previously by Refs. [50,60]; and [61] in the case of tricrin, 5-hydroxy-3,6,7,8,3',4'-hexamethoxyflavone, and hesperetin. Following the preliminary analysis, the expression of adipogenic and lipogenic key marker genes was investigated.

In accordance with the preliminary results demonstrating lipids and triglyceride accumulation, both HPMFs significantly downregulated the expression of adipogenic and lipogenic genes (PPAR $\gamma$ , C/EBP $\alpha$ , C/EBP $\beta$ , aP2, SREBF1, FASN). These genes are well-known positive regulators of adipogenesis and lipogenesis. C/EBP $\beta$  is induced early in the differentiation of adipocytes and then induces the expression of PPAR $\gamma$  and C/EBP $\alpha$ , which work cooperatively in a single pathway and are involved in the last stages of adipocyte differentiation [5,62]. Likewise, after induction of differentiation, expression of lipogenic genes (FASN, SREBF1) is also induced. FASN is known to be involved in regulating adipose tissue mass and lipid metabolism and can be considered a potential therapeutic target in the treatment of obesity [63,64]. Likewise, SREBF1 is involved in the synthesis of fatty acids and triglycerides [65]. The results obtained in this study were consistent with the previously reported anti-obesity effects of HPMFs. Previously, [48,50]; and [47] also reported similar effects of HPMFs in 3T3-L1 adipocytes. After confirming that these HPMFs possess anti-adipogenic effects, we next investigated whether they inhibit adipogenesis in the early stages (MCE phase)

of 3T3-L1 differentiation. For this experiment, the effects of these HPMFs on cell cycle-related genes (Cyclin D1, c-Myc, and cyclin A2) were investigated. As shown in Figure 12, 3'-OH-TetMF and 4'-OH-TetMF significantly enhanced the mRNA expression of c-Myc and Cyclin D1, and decreased cyclin A2 expression. Consistent with the anti-adipogenic effects, overall, the effect of 4'-OH-TetMF was higher than 3'-OH-TetMF. c-Myc and Cyclin D1 are the direct target genes of the Wnt/ $\beta$ -catenin pathway. Activation of this pathway enhances c-Myc and Cyclin D1 expression [66,67]. This indicates that these HPMFs may inhibit adipogenesis in 3T3-L1 adipocytes through activation of Wnt/ $\beta$ -catenin pathway but it requires further research.

Lastly, we investigated the effects of these HPMFs on the expression of lipolysis related genes, and secreted proteins from mature adipocytes. Lipolysis plays a crucial role in the hydrolysis of triglycerides to fatty acids and glycerol. Activation of lipolysis helps to reduce the stored fat contents in adipose tissue and thus can be a potential therapeutic pathway in obesity [68]. In adipocytes, lipolysis is achieved by the sequential action of ATGL, HSL and MGL [69]. In this study, both HPMFs significantly enhanced glycerol release (an indication of triglyceride breakdown) and lipolysis related gene expression (ATGL, HSL, and MGL). This shows that in addition to direct anti-adipogenic effects, these HPMFs also accelerate lipid catabolism. These results were in line to those reported by Refs. [70,71] in the case of acacetin (5,7-dihydroxy-3'-methoxyflavone) and apigenin (4',5,7-trihydroxy flavone). In addition, these HPMFs also significantly reduced the secretion of adipokines (TNF- $\alpha$ , IL-6, resistin, chemerin, and leptin) from mature adipocytes and enhanced adiponectin secretion. In obesogenic conditions, mature adipocytes secrete a variety of cytokines known as adipokines [72], which exert various effects on other organs and tissues. TNF- $\alpha$  and IL-6 are pro-inflammatory cytokines. TNF- $\alpha$  is the first pro-inflammatory cytokine identified to link obesity with chronic inflammation and insulin resistance [73]. Similarly, IL-6 has also been reported to cause insulin resistance and decreases insulin sensitivity [74]. In addition to their inflammatory roles, TNF- $\alpha$  has been reported to induce mitochondrial dysfunction in 3T3-L1 adipocytes [73], while IL-6 secretion is known to be in direct proportion with increased body mass, free fatty acids level and waist circumference [75]. Likewise, resistin links central adiposity to insulin resistance, and the levels of resistin are positively correlated with insulin resistance in individuals with hyper resistinemia [76,77]. Similarly, chemerin is believed to be a link between inflammation and obesity [78], mediate early stages of acute inflammation, and facilitate the differentiation and maturation of preadipocytes [79]. Likewise, leptin is multifactorial protein and is almost exclusively secreted by adipocytes. Circulating level of serum leptin is in direct relation to the total body fat mass. In obesity, leptin resistance limits its biological activity and plays a major in metabolic syndrome [80].

In contrast to other adipokines discussed, adiponectin secretion decreases in obesogenic conditions [44]. Adiponectin has anti-inflammatory, anti-diabetic, and cardioprotective effects, and thus may contribute in the development of therapies against obesity [80]. It is also involved in the regulation of fatty acid breakdown [44], and its production decreases with the increased accumulation of body fat [81]. In this study, both HPMFs significantly increased the secretion of adiponectin, which indicates that this increase might be due to the suppressive effects of these flavones on adipocyte hypertrophy.

Despite the consistent anti-obesity effects of the HPMFs investigated in the present study, we recognise some limitations due to lack of resources. The mRNA expression analysis of various genes has been investigated but the effects of these HPMFs on adipogenic, lipogenic and lipolytic transcription factors could not be investigated. In addition, cell cycle analysis could not be done through flow cytometry to fully understand the number of cells during the different stages of MCE. In future studies, the transcription factors of the genes investigated in this study should also be evaluated through Western blot and cell cycle analysis through flow cytometry to understand the mechanism of action of these HPMFs deeply. Moreover, the cell cycle genes, specifically c-Myc and

Cyclin D1 are the target genes of Wnt/ $\beta$ -catenin pathway; and it should be further investigated whether the anti-adipogenic effects of these HPMFs are through activation of the Wnt/ $\beta$ -catenin pathway.

## 5. Conclusion

In conclusion, the results obtained in the present study show that 3'-OH-TetMF and 4'-OH-TetMF possess anti-obesity effects by reducing the activity of PL in a competitive manner. In 3T3-L1 cells, they inhibit adipogenesis and lipogenesis, and enhance lipolysis through regulation of adipogenic, lipogenic and lipolytic genes (PPAR $\gamma$ , C/EBP $\alpha$ , C/EBP $\beta$ , aP2, SREBF1, FASN, ATGL, HSL, and MGL). Furthermore, the results obtained also showed that these HPMFs reduce the secretion of adipokines (including pro-inflammatory cytokines) from mature adipocytes. In addition, it is also concluded that substituting -OCH<sub>3</sub> group with -OH group at 4' position of the B ring may enhance the efficacy and overall anti-obesity effects of flavones. However, further work is needed to fully understand the structure-activity relationship and mechanism of action of these HPMFs, before their clinical approval as drugs for the treatment of obesity.

## Funding

The study was funded by Taylor's University Lake Side Campus No. 1 Jalan Taylor's, 47500 Subang Jaya, Malaysia, under Taylor's University Flagship Research Programme (TUFR), Grant Number TUFR/2017/003/05, by the UK Engineering and Physical Sciences Research Council (EPSRC) grant EP/W524177/1 and by the University of Kent's Global Challenges Doctoral Centre.

## Credit author statement

BA conceptualized the study and performed all the experimental work. EF, and CJS synthesized the HPMFs. MSV contributed to the experimental work. NK guided in the qPCR experiments and manuscript preparation. JSEL guided during molecular docking analysis. MDG, CJS, ILF, and EHW edited the manuscript and supervised the overall experimental work.

## Declaration of competing interest

The authors declare that they have no known competing financial interests or personal relationships that could have appeared to influence the work reported in this paper.

## Data availability

The data that has been used is confidential.

## References

- [1] A. Seyedan, M.A. Alshawsh, M.A. Alshagga, S. Koosha, Z. Mohamed, Medicinal plants and their inhibitory activities against pancreatic lipase: a review. Evidence-based Complement, Alternative Med. (2015), 2015.
- [2] IHME, Findings from the Global Burden of Disease Study 2017, Geneva World Heal, Organ, 2018.
- [3] T. Vos, S.S. Lim, C. Abbafati, K.M. Abbas, M. Abbasi, M. Abbasifard, M. Abbasi-Kangevari, H. Abbastabar, F. Abd-Allah, A. Abdelalim, others, Global burden of 369 diseases and injuries in 204 countries and territories, 1990–2019: a systematic analysis for the Global Burden of Disease Study 2019, *Lancet* 396 (2020) 1204–1222.
- [4] J. Li, H. Duan, Y. Liu, L. Wang, X. Zhou, Biomaterial-Based therapeutic strategies for obesity and its comorbidities, *Pharmaceutics* 14 (2022) 1445.
- [5] E.R. Nunn, A.B. Shinde, E. Zaganjor, Weighing in on adipogenesis, *Front. Physiol.* 13 (2022).
- [6] H. Dong, W. Sun, Y. Shen, M. Baláz, L. Balázová, L. Ding, M. Löffler, B. Hamilton, N. Klötting, M. Blüher, others, Identification of a regulatory pathway inhibiting adipogenesis via RSPO2, *Nat. Metab.* 4 (2022) 90–105.
- [7] K. Itoh, T. Matsukawa, T. Deguchi, M. Yamagami, N. Tomohiro, K. Murata, S. Kajiyama, Y. Endo, H. Matsuda, S. Shigeoka, others, Effective utilization of citrus

- unshiu plant waste extracts with lipase inhibitory activities, *J. Plant Stud.* 10 (2021).
- [8] G. Zhu, Q. Fang, F. Zhu, D. Huang, C. Yang, Structure and function of pancreatic lipase-related protein 2 and its relationship with pathological states, *Front. Genet.* 12 (2021) 1061.
- [9] R.B. Birari, K.K. Bhutani, Pancreatic lipase inhibitors from natural sources: unexplored potential, *Drug Discov. Today* 12 (2007) 879–889.
- [10] R.M. Jamous, S.Y. Abu-Zaitoun, R.J. Akkawi, M.S. Ali-Shtayeh, Antiobesity and antioxidant potentials of selected Palestinian medicinal plants. Evidence-based complement, *Alternative Med.* (2018) 1–21, 2018.
- [11] D.H. Kim, Y.H. Park, J.S. Lee, H. Il Jeong, K.W. Lee, T.H. Kang, Anti-obesity effect of DKB-117 through the inhibition of pancreatic lipase and  $\alpha$ -Amylase activity, *Nutrients* 12 (2020) 3053.
- [12] S.M. El-Korany, O.M. Helmy, A.M. El-Halawany, Y.E.-M. Ragab, H.H. Zedan, Kojic acid repurposing as a pancreatic lipase inhibitor and the optimization of its production from a local *Aspergillus oryzae* soil isolate, *BMC Biotechnol.* 20 (2020) 1–16.
- [13] N.A. Lunagariya, N.K. Patel, S.C. Jagtap, K.K. Bhutani, Inhibitors of pancreatic lipase: state of the art and clinical perspectives, *EXCLI J* 13 (2014) 897.
- [14] B. Ahmad, C.J. Serpell, I.F. Lim, E.H. Wong, Molecular mechanisms of adipogenesis: the anti-adipogenic role of AMP-activated protein kinase, *Front. Mol. Biosci.* 7 (2020) 76.
- [15] B. Ahmad, E.P. Friar, M.S. Vohra, M.D. Garrett, C.J. Serpell, L.L. Fong, E.H. Wong, Mechanisms of action for the anti-obesogenic activities of phytochemicals, *Phytochemistry* 180 (2020), 112513.
- [16] M.N. Evseeva, M.S. Balashova, K.Y. Kulebyakin, Y.P. Rubtsov, Adipocyte biology from the perspective of *in vivo* research: review of key transcription factors, *Int. J. Mol. Sci.* 23 (2021) 322.
- [17] P. Tang, S. Virtue, J.Y.G. Goie, C.W. Png, J. Guo, Y. Li, H. Jiao, Y.L. Chua, M. Campbell, J.M. Moreno-Navarrete, others, Regulation of adipogenic differentiation and adipose tissue inflammation by interferon regulatory factor 3, *Cell Death & Differ* 28 (2021) 3022–3035.
- [18] B. Ahmad, E.P. Friar, E. Taylor, M.S. Vohra, C.J. Serpell, M.D. Garrett, J.S.E. Loo, I. L. Fong, E.H. Wong, Anti-pancreatic lipase and anti-adipogenic effects of 5, 7, 3', 4', 5'-pentamethoxy and 6, 2', 4'-trimethoxy flavone-An *in vitro* study, *Eur. J. Pharmacol.* 938 (2023), 175445.
- [19] A.I. Owis, Citrus polymethoxyflavones: biofunctional molecules of therapeutic interest, in: *Studies in Natural Products Chemistry*, first ed., Elsevier B.V., 2019.
- [20] B. Tu, Z.-F. Chen, Z.-J. Liu, R.-R. Li, Y. Ouyang, Y.-J. Hu, Study of the structure-activity relationship of flavonoids based on their interaction with human serum albumin, *RSC Adv* 5 (2015) 73290–73300.
- [21] S. Li, M.-H. Pan, C.-Y. Lo, D. Tan, Y. Wang, F. Shahidi, C.-T. Ho, Chemistry and health effects of polymethoxyflavones and hydroxylated polymethoxyflavones, *J. Funct. Foods* 1 (2009) 2–12.
- [22] S.L. Ong, S.H. Mah, H.Y. Lai, Porcine pancreatic lipase inhibitory agent isolated from medicinal herb and inhibition kinetics of extracts from *Eleusine indica* (L.) Gaertner, *J. Pharm.* (2016), 2016.
- [23] S.L. Ong, S. Paneerchelvan, H.Y. Lai, N.K. Rao, *In vitro* lipase inhibitory effect of thirty two selected plants in Malaysia, *Asian J. Pharm. Clin. Res.* 7 (2014) 19–24.
- [24] A. Dechakhamphu, N. Wongchum, Screening for anti-pancreatic lipase properties of 28 traditional Thai medicinal herbs, *Asian Pac. J. Trop. Biomed.* 5 (2015) 1042–1045.
- [25] R.A. Friesner, R.B. Murphy, M.P. Repasky, L.L. Frye, J.R. Greenwood, T.A. Halgren, P.C. Sanschagrin, D.T. Mainz, Extra precision glide: docking and scoring incorporating a model of hydrophobic enclosure for protein-ligand complexes, *J. Med. Chem.* 49 (2006) 6177–6196.
- [26] G.K. Veeramachani, K.K. Raj, L.M. Chalasani, S.K. Annamraju, J.S. Bondili, V. R. Talluri, Shape based virtual screening and molecular docking towards designing novel pancreatic lipase inhibitors, *Bioinformation* 11 (2015) 535.
- [27] M.-P. Eglhoff, F. Marguet, G. Buono, R. Verger, C. Cambillau, H. van Tilbeurgh, The 2.46 Å resolution structure of the pancreatic lipase-colipase complex inhibited by a C11 alkyl phosphonate, *Biochemistry* 34 (1995) 2751–2762.
- [28] M.N.M. Rodhi, F. Hamzah, K.H.K. Hamid, Kinetic behaviour of pancreatic lipase inhibition by ultrasonicated *A. Malaccensis* and *A. Subintegra* leaves of different particle sizes, *Bull. Chem. React. Eng. & Catal.* 15 (2020) 818–828.
- [29] F. Hadrich, S. Sayadi, Apigenin inhibits adipogenesis in 3T3-L1 cells by downregulating PPAR $\gamma$  and CEBP- $\alpha$ , *Lipids Health Dis* 17 (2018) 1–8.
- [30] S. Kamiloglu, G. Sari, T. Ozdal, E. Capanoglu, Guidelines for cell viability assays, *Food Front* 1 (2020) 332–349.
- [31] A.K. Yadav, B.-C. Jang, Inhibition of lipid accumulation and cyclooxygenase-2 expression in differentiating 3T3-L1 preadipocytes by pazopanib, a multikinase inhibitor, *Int. J. Mol. Sci.* 22 (2021) 4884.
- [32] J. Yamaguchi, T. Tanaka, H. Saito, S. Nomura, H. Aburatani, H. Waki, T. Kadowaki, M. Nangaku, Echinomycin inhibits adipogenesis in 3T3-L1 cells in a HIF-independent manner, *Sci. Rep.* 7 (2017) 6516.
- [33] F. Castillo, D.R. González, R. Moore-Carrasco, Effects of *Phaseolus vulgaris* extract on lipolytic activity and differentiation of 3T3-L1 preadipocytes into mature adipocytes: a strategy to prevent obesity, *J. Nutr. Metab.* (2019), 2019.
- [34] I.B. Masesane, A comprehensive review of the oxidative cyclisation of 2'-hydroxychalcones to aurones and flavones, *Int. J. Chem. Stud* 3 (2015) 53–59.
- [35] W. Lan, F. Lu, M. Regner, Y. Zhu, J. Rencoret, S.A. Ralph, U.I. Zakai, K. Morreel, W. Boerjan, J. Ralph, Tricin, a flavonoid monomer in monocot lignification, *Plant Physiol* 167 (2015) 1284.
- [36] M. Cabrera, M. Simoens, G. Falchi, M.L. Lavaggi, O.E. Piro, E.E. Castellano, A. Vidal, A. Azqueta, A. Monge, A.L. de Cerain, others, Synthetic chalcones, flavanones, and flavones as antitumoral agents: biological evaluation and structure-activity relationships, *Bioorganic & Med. Chem.* 15 (2007) 3356–3367.
- [37] S.K. Hanson, R. Wu, L.A. Silks, C-C or C-O bond cleavage in a phenolic lignin model compound: selectivity depends on vanadium catalyst, *Angew. Chemie* 124 (2012) 3466–3469.
- [38] K. Okano, K. Okuyama, T. Fukuyama, H. Tokuyama, Mild debenzoylation of aryl benzyl ether with BCl<sub>3</sub> in the presence of pentamethylbenzene as a non-Lewis-basic cation scavenger, *Synlett* (2008) 1977–1980, 2008.
- [39] E. Mentese, F. Yılmaz, M. Emirik, S. Ülker, B. Kahveci, Synthesis, molecular docking and biological evaluation of some benzimidazole derivatives as potent pancreatic lipase inhibitors, *Bioorg. Chem.* 76 (2018) 478–486.
- [40] F. Carrière, K. Thirstrup, S. Hjorth, F. Ferrato, P.F. Nielsen, C. Withers-Martinez, C. Cambillau, E. Boel, L. Thim, R. Verger, Pancreatic lipase structure-function relationships by domain exchange, *Biochemistry* 36 (1997) 239–248.
- [41] S.Y. Lim, J.M. Steiner, H. Cridge, Lipases: it's not just pancreatic lipase, *Am. J. Vet. Res.* 83 (2022).
- [42] F.K. Winkler, A. d'Arcy, W. Hunziker, Structure of human pancreatic lipase, *Nature* 343 (1990) 771–774.
- [43] T.-T. Liu, X.-T. Liu, Q.-X. Chen, Y. Shi, Lipase inhibitors for obesity: a review, *Biomed. & Pharmacother.* 128 (2020), 110314.
- [44] J.Y. Je, J.E. Park, Y. Seo, J.S. Han, HM-chromanone inhibits adipogenesis by regulating adipogenic transcription factors and AMPK in 3T3-L1 adipocytes, *Eur. J. Pharmacol.* 892 (2021), 173689.
- [45] W.-Y. Song, J.-H. Choi, Korean *Curcuma longa* L. induces lipolysis and regulates leptin in adipocyte cells and rats, *Nutr. Res. Pract.* 10 (2016) 487–493.
- [46] F. Zatterale, M. Longo, J. Naderi, G.A. Raciti, A. Desiderio, C. Miele, F. Beguinot, Chronic adipose tissue inflammation linking obesity to insulin resistance and type 2 diabetes, *Front. Physiol.* 1607 (2020).
- [47] C.-S. Lai, M.-H. Ho, M.-L. Tsai, S. Li, V. Badmaev, C.-T. Ho, M.-H. Pan, Suppression of adipogenesis and obesity in high-fat induced mouse model by hydroxylated polymethoxyflavones, *J. Agric. Food Chem.* 61 (2013) 10320–10328.
- [48] D. Lee, H.Y. Park, S. Kim, Y. Park, M.-H. Bang, J.-Y. Imm, Anti-adipogenic effect of oat hull extract containing tricrin on 3T3-L1 adipocytes, *Process Biochem* 50 (2015) 2314–2321.
- [49] R. Tsutsumi, T. Yoshida, Y. Nii, N. Okahisa, S. Iwata, M. Tsukayama, R. Hashimoto, Y. Taniguchi, H. Sakaue, T. Hosaka, E. Shuto, T. Sakai, Sudachitin, a polymethoxylated flavone, improves glucose and lipid metabolism by increasing mitochondrial biogenesis in skeletal muscle, *Nutr. Metab.* 11 (2014) 1–14.
- [50] Y. Wang, P.-S. Lee, Y.-F. Chen, C.-T. Ho, M.-H. Pan, Suppression of adipogenesis by 5-hydroxy-3, 6, 7, 8, 3', 4'-hexamethoxyflavone from orange peel in 3T3-L1 cells, *J. Med. Food* 19 (2016) 830–835.
- [51] M. Łuźny, T. Tronina, E. Kozłowska, E. Kostrzewa-Susłow, T. Janeczko, Biotransformation of 5, 7-methoxyflavones by selected entomopathogenic filamentous fungi, *J. Agric. Food Chem.* 69 (2021) 3879–3886.
- [52] P. Li, Y. Zhang, Z. Wang, H. Chen, X. Li, Y. Jin, A novel flavone from the leaves of *Murraya paniculata*, *Chem. Nat. Compd.* 54 (2018) 1061–1063.
- [53] J.W. Pelley, Elsevier's Integrated Review Biochemistry E-Book: with STUDENT CONSULT Online Access, 2011.
- [54] A.K. Singh, M.K. Ekka, A. Kaushik, V. Pandya, R.P. Singh, S. Banerjee, M. Mittal, V. Singh, S. Kumaran, Substrate-induced facilitated dissociation of the competitive inhibitor from the active site of O-acyl serine sulphydrylase reveals a competitive-allosteric mechanism, *Biochemistry* 56 (2017) 5011–5025.
- [55] S.G. Patil, M.P. Patil, V.L. Maheshwari, R.H. Patil, *In vitro* lipase inhibitory effect and kinetic properties of di-terpenoid fraction from *Calotropis procera* (Aiton), *Biocatal. Agric. Biotechnol.* 4 (2015) 579–585.
- [56] F. Liang, Y. Shi, W. Cao, J. Shi, The inhibition mechanisms of pancreatic lipase by apigenin and its anti-obesity mechanisms revealed by using network pharmacology, *Food Biosci* 45 (2022), 101515.
- [57] O. Trott, A.J. Olson, AutoDock Vina: improving the speed and accuracy of docking with a new scoring function, efficient optimization, and multithreading, *J. Comput. Chem.* 31 (2010) 455–461.
- [58] V.M. Breinholt, S.E. Rasmussen, K. Brøsen, T.H. Friedberg, *In vitro* metabolism of genistein and tangeretin by human and murine cytochrome P450s, *Pharmacol. Toxicol.* 93 (2003) 14–22.
- [59] X. Huang, J. Zhu, L. Wang, H. Jing, C. Ma, X. Kou, H. Wang, Inhibitory mechanisms and interaction of tangeretin, 5-demethyltangeretin, nobiletin, and 5-demethylnobiletin from citrus peels on pancreatic lipase: kinetics, spectroscopies, and molecular dynamics simulation, *Int. J. Biol. Macromol.* 164 (2020) 1927–1938.
- [60] D. Lee, J.-Y. Imm, Antiobesity effect of tricrin, a methylated cereal flavone, in high-fat-diet-induced obese mice, *J. Agric. Food Chem.* 66 (2018) 9989–9994.
- [61] P. Subash-Babu, A.A. Alshatwi, Hesperetin inhibit adipocyte differentiation and enhance bax- and p21-mediated adipolysis in human mesenchymal stem cell adipogenesis, *J. Biochem. Mol. Toxicol.* 29 (2015) 99–108.
- [62] M. Audano, S. Pedretti, D. Caruso, M. Crestani, E. De Fabiani, N. Mitro, Regulatory mechanisms of the early phase of white adipocyte differentiation: an overview, *Cell. Mol. Life Sci.* 79 (2022) 1–14.
- [63] M.S. Choi, J.-Y. Jung, H.-J. Kim, M.R. Ham, T.R. Lee, D.W. Shin, S-nitrosylation of fatty acid synthase regulates its activity through dimerization [S], *J. Lipid Res.* 57 (2016) 607–615.
- [64] A. Czumaj, T. Śledziński, A. Mika, Branched-chain fatty acids alter the expression of genes responsible for lipid synthesis and inflammation in human adipose cells, *Nutrients* 14 (2022) 2310.
- [65] C. Liang, L. Qiao, Y. Han, J. Liu, J. Zhang, W. Liu, Regulatory roles of SREBF1 and SREBF2 in lipid metabolism and deposition in two Chinese representative fat-tailed sheep breeds, *Animals* 10 (2020) 1317.

- [66] A. Dougan, S. Demirci, H. Apdik, O.F. Bayrak, S. Gulluoglu, E.C. Tuysuz, O. Gusev, A.A. Rizvanov, E. Nikerel, F. cSahin, A new hope for obesity management: boron inhibits adipogenesis in progenitor cells through the Wnt/ $\beta$ -catenin pathway, *Metabolism* 69 (2017) 130–142.
- [67] Jongsung Lee, Jienny Lee, E. Jung, W. Hwang, Y.-S. Kim, D. Park, Isorhamnetin-induced anti-adipogenesis is mediated by stabilization of  $\beta$ -catenin protein, *Life Sci* 86 (2010) 416–423.
- [68] D. Torres-Villarreal, A. Camacho, H. Castro, R. Ortiz-Lopez, A.L. la Garza, Anti-obesity effects of kaempferol by inhibiting adipogenesis and increasing lipolysis in 3T3-L1 cells, *J. Physiol. Biochem.* 75 (2019) 83–88.
- [69] T.S. Nielsen, N. Jessen, J.O.L. Jørgensen, N. Møller, S. Lund, Dissecting adipose tissue lipolysis: molecular regulation and implications for metabolic disease, *J. Mol. Endocrinol.* 52 (2014) R199–R222.
- [70] C.-J. Liou, S.-J. Wu, L.-C. Chen, K.-W. Yeh, C.-Y. Chen, W.-C. Huang, Acacetin from traditionally used *Saussurea involucrata* Kar. et Kir. suppressed adipogenesis in 3T3-L1 adipocytes and attenuated lipid accumulation in obese mice, *Front. Pharmacol.* 8 (2017) 589.
- [71] Y.-S. Sun, W. Qu, Dietary Apigenin promotes lipid catabolism, thermogenesis, and browning in adipose tissues of HFD-Fed mice, *Food Chem. Toxicol.* 133 (2019), 110780.
- [72] X. Pu, D. Chen, Targeting adipokines in obesity-related tumors, *Front. Oncol.* 3099 (2021).
- [73] X.-H. Chen, Y.-P. Zhao, M. Xue, C.-B. Ji, C.-L. Gao, J.-G. Zhu, D.-N. Qin, C.-Z. Kou, X.-H. Qin, M.-L. Tong, others, TNF- $\alpha$  induces mitochondrial dysfunction in 3T3-L1 adipocytes, *Mol. Cell. Endocrinol.* 328 (2010) 63–69.
- [74] J.M. Harkins, N. Moustaid-Moussa, Y.-J. Chung, K.M. Penner, J.J. Pestka, C. M. North, K.J. Claycombe, Expression of interleukin-6 is greater in preadipocytes than in adipocytes of 3T3-L1 cells and C57BL/6J and ob/ob mice, *J. Nutr.* 134 (2004) 2673–2677.
- [75] K. Makki, P. Froguel, I. Wolowczuk, Adipose tissue in obesity-related inflammation and insulin resistance: cells, cytokines, and chemokines, *ISRN Inflamm* (2013), 2013.
- [76] K. Su, Y. Li, D. Zhang, J. Yuan, C. Zhang, Y. Liu, L. Song, Q. Lin, M. Li, J. Dong, Relation of circulating resistin to insulin resistance in type 2 diabetes and obesity: a systematic review and meta-analysis, *Front. Physiol.* 1399 (2019).
- [77] S. Wijetunge, R. Ratnayake, H. Kotakadeniya, S. Rosairo, K. Albracht-Schulte, L. Ramalingam, N. Moustaid-Moussa, N.S. Kalupahana, Association between serum and adipose tissue resistin with dysglycemia in South Asian women, *Nutr. \& Diabetes* 9 (2019) 1–11.
- [78] K. Zorena, O. Jachimowicz-Duda, D. Ś\kezak, M. Robakowska, M. Mrugacz, Adipokines and obesity. Potential link to metabolic disorders and chronic complications, *Int. J. Mol. Sci.* 21 (2020) 3570.
- [79] X. Su, Y. Cheng, G. Zhang, B. Wang, Chemerin in inflammatory diseases, *Clin. Chim. Acta* 517 (2021) 41–47.
- [80] K. Kowalska, A. Olejnik, J. Rychlik, W. Grajek, Cranberries (*Oxycoccus quadripetalus*) inhibit lipid metabolism and modulate leptin and adiponectin secretion in 3T3-L1 adipocytes, *Food Chem* 185 (2015) 383–388.
- [81] Y. Okabe, T. Shimada, T. Horikawa, K. Kinoshita, Suppression of adipocyte hypertrophy by polymethoxyflavonoids isolated from *Kaempferia parviflora*, *Phytomedicine* 21 (2014) 800–806.